European Journal of Medicinal Chemistry 157 (2018) 1406–1425

Contents lists available at ScienceDirect

European Journal of Medicinal Chemistry

journal homepage: http://www.elsevier.com/locate/ejmech

Review article

Copper radiopharmaceuticals for theranostic applications

Anife Ahmedova [a, *], Boyan Todorov [a], Nikola Burdzhiev [a], Christine Goze [b, **]

[a] Faculty of Chemistry and Pharmacy, Sofia University, 1, J. Bourchier av., 1164, Sofia, Bulgaria
[b] Institut de Chimie Moléculaire de l'Université de Bourgogne (ICMUB), UMR CNRS 6302, P2DA Team, Université de Bourgogne, 21000, Dijon, France

ARTICLE INFO

Article history:
Received 25 January 2018
Received in revised form
15 August 2018
Accepted 18 August 2018
Available online 23 August 2018

Keywords:
Copper radionuclides
Theranostics
Radiopharmaceuticals
Radioimaging
Radiotherapy
Copper chelators

ABSTRACT

The growing advancement in nuclear medicine challenges researchers from several different fields to integrate imaging and therapeutic modalities in a theranostic radiopharmaceutical, which can be defined as a molecular entity with readily replaceable radioisotope to provide easy switch between diagnostic and therapeutic applications for efficient and patient-friendly treatment of diseases. For such a reason, the diagnostic and therapeutic potential of all five medical radionuclides of copper have thoroughly been investigated as they boost the hope for development of successful radiotheranostics. To facilitate the mutual understanding between all different specialists working on this multidisciplinary field, we summarized the recent updates in copper-based nuclear medicine, with specific attention to the potential theranostic applications. Thereby, this review paper is focused on the current achievements in the copper-related complementary fields, such as synthetic and nuclear chemistry, biological assessment of radiopharmaceuticals, design and development of nanomaterials for multimodal theranostic implications. This work includes: i) description of available copper radionuclide production methods; ii) analyses of the synthetic strategies for development of improved copper radiopharmaceuticals; iii) summary of reported clinical data and recent preclinical studies from the last five years on biological applicability of copper radiopharmaceuticals; and iv) illustration of some sophisticated multimodal nanotheranostic agents that comprise several imaging and therapeutic modalities. Significant advancement can be seen in the synthetic procedures, which enables the broader implication of pretargeting approaches via bioorthogonal click reactions, as well as in the nanotechnology methods for biomimetic construction of biocompatible multimodal copper theranostics. All this gives the hope that personalized treatment of various diseases can be achieved by copper theranostics in the near future.

Contents

* Corresponding author.
** Corresponding author.
E-mail addresses: ahmedova@chem.uni-sofia.bg (A. Ahmedova), Christine.Goze@u-bourgogne.fr (C. Goze).

https://doi.org/10.1016/j.ejmech.2018.08.051
0223-5234/

1. Introduction

The emerging trend in medicine, termed as personalized medicine, advances beyond genomics and evermore implies the medical imaging to consider the patient's genetic, anatomical and physiological characteristics as the best way for personalized medical treatment. This imposes specific requirements for both the visualization techniques and the imaging probes, which have to provide high-resolution anatomical images with physiological information and be equally appropriate for diagnostics and therapy. Basic imaging tools of medical diagnostics, which are daily used to acquire important information about diseases stage and localization, are computed tomography (CT), magnetic resonance imaging (MRI), single-photon emission computed tomography (SPECT), and positron emission tomography (PET). Nowadays, the use of dual modalities, such as PET/CT and SPECT/CT, enables the scientists and clinicians to identify the physiological basis of disease and correlate it with the anatomical image [1]. Thereby, new and more ambitious tasks of modern medicine have been defined requiring also advanced therapeutic approaches. Such an example is the radiotheranostic treatment that aims at targeting, imaging and treating tumors by the use of one and the same molecular structure in which the radioisotope is easily replaceable. While this new branch of nuclear medicine provides a universal tool in the hands of physicians, it also implies rather specific requirements to the radioisotopes and their chemical or biochemical carriers that are the subject of increased research in the last years. Selection of proper radionuclide for radiotheranostics is critical and requires the following properties: i) appropriate half-life (close to residence time of the radiopharmaceutical in the organism); ii) existence of different decay schemes or isotope pairs that are suitable for both imaging and therapy; iii) lack of high-energy gamma emission (to limit the personal dose overload); iv) suitable radiochemistry allowing mild labeling condition and high *in vivo* stability; and v) availability of the isotopes (related to production site and cost efficiency). All these requirements make the metal radioisotopes increasingly popular for theranostic applications among the available radionuclides [2]. As such, copper isotopes represent an excellent choice for theranostics due to the large variety of half-lives they provide (from 0.16 to 62.01 h) and their decay properties (β^+, β^-, or EC), which are suitable for diagnostic imaging, radiotherapy, or both for imaging and therapy. As a matter of comparison, the ^{18}F-radionuclide – accepted as the "gold standard" for PET imaging – has a lifetime of 1.83 h and is produced on a cyclotron, and the generator-produced ^{68}Ga isotope is a pure positron emitter with a half-life of 1.13 h [2]. Another advantage of radio-copper is the existence of considerable knowledge on the coordination and bioinorganic chemistry of copper ions that has enabled the development of highly target-specific copper complexes for predefined multimodal medical applications. Major issues regarding the stability, reactivity and redox properties of copper complexes in biological environment have been addressed in view of their application in nuclear medicine, e.g. the required high *in vivo* stability prompted the exploration of stable Cu(II) complexes resistant to transchelation as superior to Cu(I) ones, whereas the biological reduction of Cu(II) to Cu(I), leading to fast transchelation and accumulation of Cu(I), has been employed for hypoxia targeting and imaging [3,4]. Numerous interdisciplinary studies on the design and application of copper radiopharmaceuticals, suitably chelated with bifunctional chelators (BFCs), have appeared in the last decade [3,4].

A basic challenge for nuclear medicine is the need of radiopharmaceuticals that can selectively target a specific site in the human body (systems, organs or cells). There are several strategies to design and develop selective radiopharmaceutical agents. Some of the most popular strategies concern the use of elements with high natural affinities for given target organs, e.g. iodine – for the thyroid, strontium – for bones, or employ the bifunctional approach to link a target-specific molecular fragment with a radionuclide bearing site. The latter approach, however synthetically more demanding, ensures a better specificity and is nowadays used in radioimmunotherapy to link the therapeutic radionuclide with a specific antibody [4]. Dosimetry is another major task in radioimmunotherapy that requires measuring the amount of radioactivity bound to tumor cells *in vivo*, which strongly depends on the cancer type, the targeting moiety, and many other factors. Using positron-emitting copper isotopes PET images can be obtained, allowing for quantification of the radioactivity uptake. By simply changing the copper isotope with a radiotherapeutic one, and using the same biomolecular vector to transport it to tumor cells, not only the therapeutic modality can be triggered but also the quantity of radioactivity reaching the tumor (the therapeutic dose) can be defined. The possibility to conveniently combine or interchange the therapeutic and diagnostic applications of the local radiation that is provided by the available variety of copper isotopes, is the main driving force in the currently expanding research in the field of copper-based nuclear medicine. The aim of the current review paper is to outline the recent achievements in the design of copper radiopharmaceuticals, focusing on the last five years, and to highlight the new trends in engineering copper complexes for theranostic applications. While summarizing the results from joint efforts of specialists in different fields (radiochemistry, synthetic and medicinal chemistry), we will attempt to point out the established physical, chemical and biochemical requirements that apply for potentially successful copper-based radiotheranostic candidates.

2. Production and properties of copper radioisotopes

Copper has 32 isotopes, of which ^{63}Cu and ^{65}Cu are stable with natural abundances of 69.17 and 30.83%, respectively. Among the copper radionuclides, 21 have very short half-lives (less than a second), and only five of the longer-lived isotopes meet the requirements of nuclear medicine – ^{60}Cu, ^{61}Cu, ^{62}Cu, ^{64}Cu and ^{67}Cu. Basic nuclear properties of these isotopes, which define the potential areas of their medicinal applications, are summarized in Table 1 [5,6]. Based on their half-lives, the Cu isotopes can be separated into two groups: short-lived ^{62}Cu and ^{60}Cu and the long-lived ^{61}Cu, ^{64}Cu and ^{67}Cu isotopes. The first group is particularly adapted to image fast processes in living organisms (such as myocardial and renal perfusion), whereas the second group is appropriate to study slower processes that require accumulation of the targeting agents. The classification of Cu isotopes according their decay modes is used to suggest them as visualization agents (positron emitters ^{60}Cu, ^{61}Cu, ^{62}Cu and ^{64}Cu) or radiotherapeutics (beta emitters ^{64}Cu and ^{67}Cu). The other two characteristics that define the applicability of copper isotopes are their way of production, which determine their cost and availability, and the linear energy distribution that is related to the average tissue penetration lengths.

^{60}Cu, as a β^+ (positron) emitter is suitable tracer for PET, although it has the disadvantage of concomitant γ emission [7]. It can be produced on a medical cyclotron at relatively low cost using proton- or deuteron-induced reactions on ^{60}Ni-enriched targets. ^{60}Cu is a proton-rich nuclide that decays to its stable Ni isotopes through a combination of positron decay and electron capture (EC) processes [8,9].

^{61}Cu isotope is a better choice for prolonged imaging of processes with slower kinetics due to its longer half-life (3.33 h) than that of ^{60}Cu and ^{62}Cu. It can be mainly produced from Ni targets [9],

Table 1
Properties of radioactive copper isotopes.

Isotope	Half-life	Decay (%)	Major radiation (%) [keV]	Average tissue penetration	Source	Production reactions	Application
^{60}Cu	23.70 min	β^+ (93) EC (7)	β^+ 1980.5 (49) γ 1333 (88)	4.4 mm	Cyclotron	^{60}Ni(p,n)^{60}Cu	radioimaging
^{61}Cu	3.33 h	β^+ (62) EC (38)	β^+ 1215.2 (51) γ 283 (12) γ 656 (11)	2.6 mm	Cyclotron	^{61}Ni(p,n)^{61}Cu	radioimaging
^{62}Cu	9.67 min	β^+ (98) EC (2)	β^+ 2926 (97)	6.1 mm	Generator Cyclotron	^{62}Zn/^{62}Cu ^{62}Ni(p,n)^{62}Cu	radioimaging
^{64}Cu	12.70 h	β^+ (19) EC (41)	β^+ 653.1 (17) γ 1346	0.7 mm	Reactor	^{nat}Zn(p,xn)^{64}Cu ^{63}Cu(n,γ)^{64}Cu	radioimaging;
		β^- (40)	β^- 578.7 (39)	0.95 mm	Cyclotron	^{64}Ni(p,n)^{64}Cu ^{64}Ni(d,2n)^{64}Cu	radiotherapy
^{67}Cu	2.57 d (62.01 h)	β^- (100)	β^- 395 (50)	0.61 mm	Reactor Cyclotron	^{67}Zn(n,p)^{67}Cu ^{68}Zn(p,2p)^{67}Cu ^{70}Zn(p,α)^{67}Cu	radiotherapy

but also from Zn or Co targets [10,11], on a medical cyclotron using proton-, deuteron- or alpha-induced reactions. The biomedical use of ^{61}Cu, however, is limited due to the necessity of highly enriched Ni targets or high-energy particle beams.

^{62}Cu is an almost pure β^+ emitter (98%) with a short half-life of 9.7 min. It is an attractive isotope because it can be produced either on a medical cyclotron, using proton- or deuteron-induced reactions on ^{62}Ni-enriched targets, or through a ^{62}Zn/^{62}Cu generator system. The mother nuclide ^{62}Zn, needed for the generator, is currently produced by proton-induced reactions on natural copper [8]. This is the preferred option for practical use in medical centers having no cyclotron. Large-scale production of the ^{62}Zn/^{62}Cu generator has been established for shipments to PET centers [12], but clinical studies on further improvements are still in progress to eventually enable the commercial distribution of this technology in the near future.

^{64}Cu is the most studied radioisotope, as it is ideal for high-resolution PET imaging and for radiotheranostics due to its low positron energy with short average tissue penetration range. It decays by three processes – electron capture, positron and beta decays. Currently, the most common production method for ^{64}Cu utilizes the ^{64}Ni(p,n)^{64}Cu reaction in a cyclotron [13,14]. The target for producing ^{64}Cu is enriched ^{64}Ni (99.6%), which is prepared (typically 10–50 mg) and electroplated onto a gold disk [15]. After bombardment, the ^{64}Cu is separated from the nickel target in a one-step procedure using an ion exchange column. The enriched ^{64}Ni can be recovered up to 85–95% and reused for future bombardments, which makes this method of ^{64}Cu production highly cost-efficient [16]. Another method of ^{64}Cu production utilizes the ^{64}Zn(n,p)^{64}Cu reaction and requires nuclear reactor and fast neutrons to bombard the target. Unfortunately, one of the byproducts of this production method is the radioactive ^{65}Zn ($T_{1/2} = 245$ d), which limits its practicality [17,18].

It should be noted that the spatial resolution of PET images obtained with ^{60}Cu, ^{61}Cu, ^{62}Cu and ^{64}Cu isotopes is in the same range or even better than the ones obtained with ^{68}Ga isotope, as can be deduced from the basic fundamental radiation properties of these isotopes (energy and intensity of emitted β^+ and γ) [8,19]. Moreover, the estimated radiation safety of ^{61}Cu, ^{62}Cu and ^{64}Cu isotopes is comparable, or even superior (^{61}Cu and ^{64}Cu), to ^{68}Ga and the gold standard in PET imaging – fluorine-18 [19].

The low positron energy of ^{64}Cu, and the subsequent short average penetration range in tissues, makes it unique among the Cu isotopes. Moreover, the absence of significant additional gamma decays renders ^{64}Cu ideal for high-resolution preclinical PET imaging and radiotheranostics. The lower branching ratio of ^{64}Cu than that of ^{18}F can be regarded as an unfavorable feature, since it would require 5.5 times higher activity (i.e. higher doses) when using ^{64}Cu instead of ^{18}F in order to obtain the same image quality. On the other hand, however, the low branching ratio of ^{64}Cu leads to 10 times lower radiotoxicity for ^{64}Cu than the more conventional radionuclide ^{18}F if we correctly estimate the excess dose delivered to the patient taking into account the biodistribution of the compound, the energy of the positron and the gamma rays, and the overall radiotoxicity [20]. Some of these limitations can actually turn into beneficial properties, in terms of lower radiotoxicity and radiation safety, which enable the use of ^{64}Cu for diagnostics and therapy, despite the significantly higher doses needed for the therapeutic application. The potential dual use of ^{64}Cu for PET imaging and radiotherapy allows to define the therapeutic dose by measuring the *in vivo* amount of radioactivity bound to the tumor cells, which strongly depends on the kind of cancer, the biomolecular vector, *etc*., and thereby overcomes a major problem in radioimmunotherapy.

Furthermore, the existence of radionuclide pairs of copper with ideal properties for imaging and radiotherapy makes it the radiometal of choice for the development of theranostic pharmaceuticals.

^{67}Cu is the longest lived copper radioisotope and due to its interesting decay properties it is potentially useful for radioimmunotherapy. Indeed, it emits β^- (beta) particles and γ rays (93 keV, 35%; 185 keV, 45%) with a half-life of 2.6 days, making it suitable for both radiotherapy and SPECT imaging [21]. However, its production method is the most difficult one as it requires fast neutron flux reactor or high-energy proton beams along with the costly ^{68}Zn target. Therefore, there are only a few biological studies using this radioisotope, unlike the other copper radionuclides. Therapeutic amounts of ^{67}Cu can be produced via several reactions on Zn. The ^{68}Zn(p,2p)^{67}Cu reaction requires increasing proton energy, from 20 to 70 MeV, and chemistry station. The ^{70}Zn(p,α)^{67}Cu reaction utilizes a low energy proton beam, 20 MeV, and therefore does not coproduce large amounts of other radioisotopes, in contrast to other production methods. The most commonly used reaction to produce ^{67}Cu is ^{67}Zn(n,p)^{67}Cu reaction due to its simplicity to perform in a nuclear reactor [22,23].

3. Design and synthesis of copper radiopharmaceuticals

The best copper radiopharmaceutical must ensure high selectivity of accumulation of the copper radionuclide in the target tissues or organs with minimum non-selective uptake in the healthy ones. This can be achieved by an efficient chelator that forms radiocopper complexes with high *in vivo* stability and high kinetic inertness, in order to avoid Cu(II) transchelation to bioavailable molecules. The efficient targeting is usually achieved by linking the chelator with a (bio)molecular vector, such as peptide, protein, and

antibody, which selectively carries the radionuclide to the specific cells of organs or tissues. This approach utilizes bifunctional chelators (BFCs), composed of metal complexing ligand and a functional group for easy covalent linking with the biomolecular vector [4,16]. Several excellent reviews have recently summarized the major characteristics of copper chelators most commonly used in metallo-radiopharmaceuticals [3,4,24–26], and therefore we shall only delineate the historical progress and advancement in the development of copper BFCs. The copper chelators that had been used in recent biological studies are summarized in the next section and are depicted in Fig. 1.

Initially, the most frequently used chelators for copper radionuclides were the acyclic ligands ATSM and PTSM due to the rapid complexation under mild conditions they provide. This is essential for facile radiolabeling, especially for short-lived isotopes, and therefore the 1,2-bis(thiosemicarbazonato) family has been extensively evaluated for its utilization in copper radiopharmaceuticals [27]. That is why, some of the most studied radio-copper complexes are the Cu(ATSM) and Cu(PTSM) that have progressed to clinical trials in humans and are recognized as ideal tracers for hypoxia and myocardial blood flow, respectively. Selective hypoxia imaging by the Cu(ATSM) complexes is achieved by the reductive retention mechanism that enables tissue retention of the radioisotope after reduction of Cu(II) to Cu(I) [28]. To fully take advantage of the rapid radiolabeling, intense research continues to improve the acyclic ligands through increasing their denticity, fine tune their lipophilicity or the backbone rigidity – all aiming at better *in vivo* stability and appropriate biodistribution of their copper complexes. Considerable achievements have been obtained with the hexadentate ligands developed by Orvig and coworkers [29,30], and the penta- or hexadentate ligands based on bicyclic bispidine [31–33] or triaminocyclohexane cores [34,35].

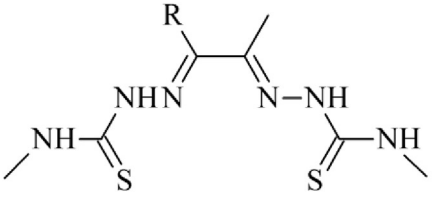

R = CH_3 - **ATSM** R = H - **PTSM**

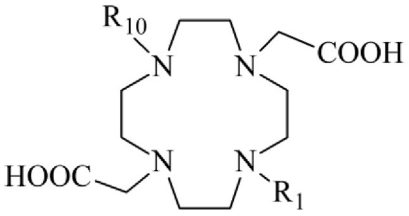

$R^1 = R^{10} = CH_2COOH$ - **DOTA**
DOTA N-hydroxysuccinimide ester - **DOTA-NHS**
R^1 = (glutaric acid)-2-yl; $R^{10} = CH_2COOH$- **DOTAGA**
$R^1 = R^{10} = -(CH_2)_2$- bridge N1,N7; - **CB-DO2A**

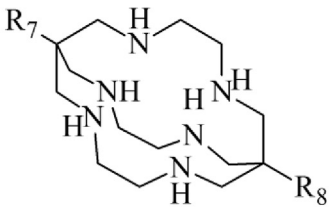

$R^7 = R^8$ = H - **Sar** (sarcophagine)
$R^7 = CONH_2$; $R^8 = CONHCH_2C_6H_4NH_2$ - **SarAr**
$R^7 = CH_3$; $R^8 = NHCO(CH_2)_3COOH$ - **MeCOSar**

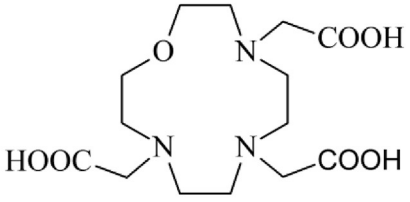

Oxo-DO3A

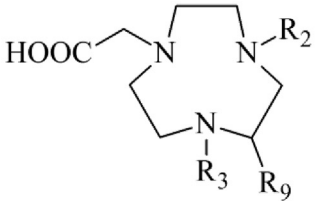

$R^2 = R^3 = CH_2COOH$; R^9 = H - **NOTA**
$R^2 = CH_2COOH$; R^3 = H or clickable group; R^9 = H - **NO2A**
$R^2 = CH_2COOH$; R^3 = (glutaric acid)-2-yl; R^9 = H - **NODAGA**
$R^2 = R^3$ = 2-pyridylmethyl; R^9 = H - **DMPTACN-COOH**
$R^2 = CH_2COOH$; R^3 = 2-((carboxymethyl)(3-(4-isothiocyanatophenyl) propyl)-amino)ethyl; R^9 = H - **p-SCN-PhPr-NE3TA**
$R^2 = R^3 = CH_2COOH$; $R^9 = CH_2NH_2$ - **MANOTA**

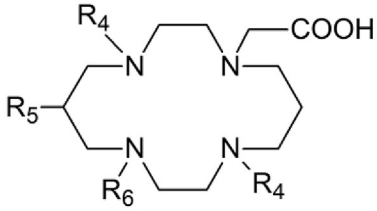

$R^4 = R^6 = CH_2COOH$; R^5 = H - **TETA**
$R^4 = R^6 = CH_2COOH$; R^5 = p-(bromoacetamido)benzyl - **BAT**
$R^4 = -(CH_2)_2$- bridge N1,N8; $R^6 = CH_2COOH$; R^5 = H - **CB-TE2A**
$R^4 = -(CH_2)_2$- bridge N1,N8; $R^6 = CH_2PO_3H_2$; R^5 = H- **CB-TE1A1P**
$R^4 = -(CH_2)_3$- bridge N1,N8; $R^6 = CH_2PO_3H_2$; R^5 = H- **PCB-TE1A1P**
R^4 = pyridine-2,6-diylbis(methylene) bridge N1,N8; $R^6 = R^5$ =H - **pycup**

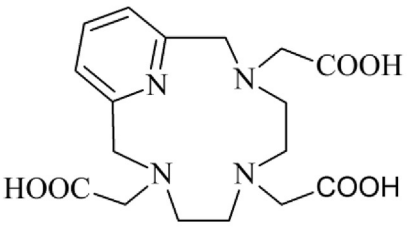

PCTA

Fig. 1. Molecular formula of the most commonly used copper chelators and their abbreviations.

Nowadays, the focus shifts towards the polyazamacrocyclic chelators due to the enhanced kinetic inertness and thermodynamic stability of their copper complexes. Tetraazamacrocyclic cyclen and cyclam ligands with pendant carboxylic arms (DOTA and TETA) have thoroughly been studied for their application as chelators in metallopharmaceuticals due to the fact that they benefit from the macrocyclic and chelate effects, thereby forming very stable complexes. The well-established use of DOTA bifunctional chelators for Sc(III), In(III), Lu(III), and Y(III) radiopharmaceuticals has triggered extensive studies on the *in vivo* applicability of DOTA chelators also for radio-copper ions, in order to estimate the quality of the corresponding Cu(II) complexes for diagnostic imaging or radiotherapy (See Table 2). While both tetraazamacrocyclic ligands are superior to the acyclic chelators in terms of kinetic inertness and thermodynamic stability of their Cu complexes, TETA complexes exhibit better resistance to acid dissociation and *in vivo* transchelation [36,37]. Nevertheless, comparative *in vivo* PET-imaging studies on biodistribution and effective clearance have concluded that DOTA and TETA are not the best chelators to be used for medical radio-copper, which have prompted the development of smaller size triazacyclononanes (NOTA), and the bicyclic tetraazamacrocycles (cross-bridged analogues of DOTA and TETA) and hexaazamacrocycles (sarcophagines) as more suitable BFCs for Cu(II) (*vide infra*) [26]. Another major drawback of DOTA and TETA chelators is that they require longer time to chelate Cu(II) ions and usually harsh conditions (25–90 °C for ~ 60 min), which can be limiting factor for some bioconjugation procedures. Therefore, intense research continues to further modify the macrocyclic backbone or change the side arms, so that the charge and hydrophilicity of the formed Cu(II) complexes can be adjusted to the required biodistribution [38–40]. Some of these modifications include attachment of one or two methylthiazolyl arms to the cyclam backbone [39], two picolinate pendant arms to cyclen [40], or formation of monopicolinates of cyclam and cyclen [41]. ^{64}Cu-complexes of DOTA ligands with several methanephosphonate pendant arms have shown higher stability constants than the Cu-DOTA complexes and high stability in rat serum. The observed high accumulation in bone has been explained with the expected binding of the methanephosphonate groups to hydroxyapatite, and therefore, the studied series of methanephosphonate macrocyclic ligands has been suggested as potentially useful for bone-imaging agents [42].

Significant improvement in radiolabeling efficiency under mild conditions (>95% at RT for 5 min) of DOTA analogues has been achieved by replacing one of the N-donor atoms of the macrocycle with an O-donor (e.g. Oxo-DO3A) or with a heterocyclic pyridine N-atom incorporated in the macrocycle (in 3,6,9,15-tetraazabicyclo [9.3.1]pentadeca-1(15),11,13-triene-3,6,9-triacetic acid, PCTA), which also ensured high *in vitro* stability as observed in their C-connected p-NO_2-benzyl bifunctional conjugates [43]. These findings have initiated several comparative studies on the performance of bombesin-linked bifunctional chelators, demonstrating also higher *in vivo* stability of PCTA-conjugate over DOTA and Oxo-DO3A [44]. Similarly, promising *in vitro* data were obtained for an RNA aptamer conjugate of PCTA showing also that the high affinity to prostate cancer-specific cell-surface antigen is not affected by the chelator [45]. Bioconjugation with certain monoclonal antibodies (MAbs) indicated more promising applicability of PCTA in comparison with other acyclic and macrocyclic chelators [46,47]. All these data have led to the recent demonstration of theranostic application of anti-EGFR antibody (cetuximab) labeled with ^{64}Cu/^{177}Lu using the PCTA as identical chelator for immuno-PET imaging and radioimmunotherapy. Thereby, the convertible diagnostic and therapeutic radiopharmaceutical ^{64}Cu-/^{177}Lu-labeled PCTA-cetuximab was suggested as both diagnostic tool in patient selection and radioimmunotherapy agent in EGFR-positive ESCC (esophageal squamous cell carcinoma) tumors [48].

The known fact that the structurally reinforced macrocycles, cross-bridged cyclam and cyclen ligands developed by Weisman and coworkers [49,50], form highly stable complexes with Cu(II) that are resistant to dissociation in strong acid have motivated their application for radio-copper chelation. Ethylene cross-bridged (CB) cyclam and cyclen derivatives (CB-TE2A and CB-DO2A) provide better kinetic properties and biological stability *in vivo* of their Cu(II) complexes than the unbridged analogues, and [^{64}Cu]Cu-CB-TE2A is superior to [^{64}Cu]Cu-CB-DO2A in this respect [51]. Archibald and coworkers have developed a series of cross-bridged and side-bridged cyclam derivatives, demonstrating ultrahigh stability of the formed Cu(II) complexes with some of the studied bifunctional chelators based on CB-TE2A analogues [52–54]. Representative crystal structure of Cu(II) complex with unsymmetrically functionalized CB-TE2A is depicted in Fig. 2. The confirmed high *in vivo* stability of Cu(II) complexes with CB-TE2A derivatives suggested this chelator as the most suitable tetraazamacrocyclic BFCs for radio-copper, which motivated numerous studies on proving the implication of CB-TE2A for radiolabeling of biomolecular vectors with copper isotopes for theranostic use. A cross-bridged cyclam derivative (CB-TE2A) with pendant *N*-succinimide group conjugated with the integrin $\alpha_v\beta_3$-binding peptide c(RGDfK(S)) has been developed by Brechbiel and coworkers and demonstrated high *in vitro* stability with no evidence for transchelation of ^{64}Cu in human serum for up to 48 h [55]. Anderson and coworkers evaluated the ^{64}Cu-complexes of a series of ethylene cross-bridged cyclam derivatives with different pendant arms, forming complexes of different charges, for their stability and biodistribution in rats. The neutral complex with the ligand bearing two carboxymethyl arms exhibited rapid clearance from all tissues and has been suggested as a significant chelator for radiolabeling with copper for diagnostic imaging and targeted radiotherapy [56]. Comparative study on [^{64}Cu]Cu-CB-TE2A-Y3-TATE and [^{64}Cu]Cu-TETA-Y3-TATE indicated that CB-TE2A is a superior bifunctional chelator for ^{64}Cu due to improved clearance from healthy organs and higher target-specific uptake by the SSTR2-positive pancreatic carcinoma cells (AR42J) in rats [57]. Since it has been pointed out that radiolabeled SSTR2 antagonists may be superior to agonists for imaging SSTR2-positive tumors, a new SSTR2 antagonist radiopharmaceutical, [^{64}Cu]Cu-CB-TE2A-sst2-ANT, was developed and a comparative study demonstrated its better tumor-to-blood and tumor-to-muscle ratios than the [^{64}Cu]Cu-CB-TE2A-Y3-TATE, and excellent tumor-to-background contrast at 4 h postinjection [58]. These initial biological data expanded significantly and some of the most recent examples on using CB-TE2A in different bioconjugation strategies for development of copper radiopharmaceuticals are listed in Table 2. The continuing efforts to improve the properties of cross-bridged cyclen derivatives (CB-DO2A) include replacing either the pendant arms or the type of the cross-bridges, or both. Cyclen-based metal chelators, containing two trans 2-hydroxybenzyl (HB) pendant arms, with and without ethylene cross-bridge have been compared and, surprisingly, showed that the copper complex of the cross-bridged cyclen derivative is 4 times less inert than the complexes of the non-bridged cyclen and its derivatives [59]. In another approach to improve the Cu(II) complexation properties of cross-bridged cyclens, Denat and coworkers introduced dibenzofuran or diphenyl ether as cross-bridging moieties, while the pendant arms remained two N-acetic acids. In this way, the kinetic inertness of the formed complexes and selectivity for Cu(II) ions significantly improved, however, the conditions for complex formation still needed further refinement for efficient labeling with copper radionuclides [60]. Certain success in the utilization of a cross-bridge bearing a donor atom, e.g. a

Table 2
Summary of the biological studies on copper-based radiopharmaceuticals.

Nuclide	Chelator- targeting biovector	Biological Target	Type of application	Type of study and comments	Ref.
^{60}Cu	ATSM	hypoxia	PET	**Clinical studies** on patients with NSCLC;	[100]
				15 patients with cervical cancer;	[101]
				38 women with cervical cancer	[102]
^{62}Cu	ATSM	hypoxia	PET	**Clinical studies** on 30 patients with HNC;	[103]
				25 patients with HNC;	[104]
				patients with glioma	[105,106]
^{62}Cu	PTSM	myocardial perfusion	cardiac imaging PET	**Clinical studies** on 68 patients to confirm the use of ^{62}Zn/^{62}Cu generator;	[107]
				45 patients with occlusive coronary artery disease	[108]
^{62}Cu	ATSM and PTSM	hypoxia and perfusion	PET visualization	**Clinical studies** on 2 patients with lung neoplasms;	[109]
				10 patients to evaluate lung masses	[110]
^{64}Cu	[^{64}Cu]$CuCl_2$	prostate cancer (PC); brain tumors	PET/CT	**Clinical studies** on 7 patients with PC;	[112]
				19 patients with cerebral tumor	[113]
^{64}Cu	[^{64}Cu]$CuCl_2$	CTR1 melanoma	PET & treatment	***in vitro* & *in vivo*** theranostic management of melanoma	[114]
^{64}Cu	ATSM	tumor hypoxia (solid tumors)	PET & PET/CT	**Clinical studies** on10 patients with cervical carcinoma;	[115]
				18 patients with NSCLC	[116]
^{64}Cu	TP3805	VPAC1 receptors	PET breast and prostate cancer	**Clinical studies** on 19 women with breast cancer;	[117]
				25 patients with PC	[118]
^{64}Cu	PTSM based ligands	amyloid-β plaques	PET of Alzheimer's disease	***in vivo* & *ex vivo*** in post-mortem human brain tissue and wild-type mice	[119]
^{64}Cu	TETA-OC	SSTR -positive tumors	PET of NETs	**Clinical studies** on 8 patients with NETs	[120]
^{64}Cu	TETA-OC (TETA-octreotide)	SSTR-positive tumors	targeted radiotherapy	***in vivo*** pancreatic tumors in Lewis rats	[121]
^{64}Cu	TETA-Y3-TATE	somatostatin analogue	targeted radiotherapy	***in vivo*** in CA20948 tumor-bearing rats	[122]
^{64}Cu/^{67}Cu	TETA-BN	bombesin (BN) receptors positive tumors	PET imaging & targeted radiotherapy	***in vivo*** PC-3 tumors	[123]
^{64}Cu	DOTA-$VEGF_{121\ or\ DEE}$	VEGFR-2-expressing 4T1 tumors	PET of tumor angiogenesis	***in vitro* & *in vivo*** in orthotopic 4T1 murine breast tumor models	[124]
^{64}Cu	DOTA-RGD	$\alpha_v\beta_3$ integrin RGD	microPET	***in vitro* & *in vivo*** in orthotopic MDA-MB-435 breast cancer model	[125]
^{64}Cu	DOTA- RGD4	$\alpha_v\beta_3$ integrin RGD4	PET of angiogenesis and teratoma formation	***in vitro* & *in vivo*** visualization of human embryonic stem (hES) cell −derived teratomas	[126]
^{64}Cu	DOTA-NGR	CD13/aminopeptidaseN (APN) receptor	microPET imaging of angiogenesis	***in vitro* & *in vivo*** in CD13-positive HT-1080 tumor xenografts	[127]
^{64}Cu	DOTA-GX1 peptide	tumor vasculature	microPET imaging	***in vitro* & *in vivo*** in U87MG tumor xenografted mouse model	[128]
^{64}Cu	DOTA-NT-Cy5.5	neurotensin receptors (NTRs)	PET of tumor	***in vitro* & *in vivo*** in HT-29 model	[129]
^{64}Cu	DOTA-ZD- G1 or G2	kinase inhibitor - vandetanib (ZD6474)	Small-animal PET	***in vitro* & *in vivo*** in U-87 MG tumor-bearing mice	[130]
^{64}Cu	tetrac/DOTA-liposomes	angiogenesis, $\alpha_v\beta_3$ integrin	PET imaging	***in vitro* & *in vivo*** in U87MG tumor-bearing mice	[131]
^{64}Cu	DOTA-TATE-PEGylated liposomes	Somatostatin receptors (SSTRs)	PET imaging of tumor	***in vitro* & *in vivo*** in neuroendocrine tumor (NET) xenograft mouse model (NCI−H727)	[132]
^{64}Cu	DOTA-h173	Axl expression in human lung cancer	microPET imaging	***in vitro* & *in vivo* & *ex vivo*** in Axl-positive A549 tumors	[133]
^{64}Cu	DOTA-anti-CTLA-4 MAb	CTLA-4 expression in tumor	PET	***in vitro* & *in vivo*** in CT26 tumor-bearing BALB/c mice	[134]
^{64}Cu	DOTA-MAb159 antibody	GRP78 receptor on cell surfaces	PET imaging	***in vitro* & *in vivo*** in BXPC3 pancreatic cancer xenografted athymic nude mice	[135]
^{64}Cu	NODAGA-trastuzumab	HER2	PET/CT	***in vitro* & *in vivo*** in mice with HER2 expressing SK-OV-3 ovarian adenocarcinoma	[136]
^{64}Cu	DOTA-rituximab	huCD20	micro-PET/CT	***in vitro* & *in vivo*** good manufacturing practices (GMP) validation for imaging B cell NHL	[137]
^{64}Cu	DOTA-$FN3_{CD20\ or\ WT}$ - human fibronectin type 3	huCD20 in B cell NHL	PET imaging of CD20	***in vitro* & *in vivo*** in Ramos cell xenografted mice	[138]
^{64}Cu	acetate and DOTA-cetuximab	EGF receptor-positive tumors	Radioimmu-notherapy	***in vitro* & *in vivo*** in KRAS-mutated HCT116 tumor-bearing mice	[140]
^{64}Cu	DOTA-anti-mouse PECAM-1 antibody	elevated expression of PECAM-1	PET of myocardial infarction	***in vitro* & *in vivo*** in a mouse model	[141]
^{64}Cu	DOTA anti-P-selectin MAb	atherosclerotic plaques	PET/CT imaging	***in vitro* & *in vivo* & *ex vivo*** excised aortas, atherosclerotic mice	[142]
^{64}Cu		targeting parenchymal Amyloid-β (Aβ) or M31		***in vitro* & *in vivo* & *ex vivo*** in TgCRND8 mouse model of Alzheimer's disease	[143]

(*continued on next page*)

Table 2 (*continued*)

Nuclide	Chelator- targeting biovector	Biological Target	Type of application	Type of study and comments	Ref.
	DOTA-NHS and a Rapp Polymer; anti-Aβ antibodies		noninvasive PET imaging of Aβ pathology		
^{64}Cu	DOTA- anti-ICAM antibody NPs	intercellular adhesion molecule 1 (ICAM-1)	PET and CT of lung endothelium	***in vitro & in vivo*** in mice models of respiratory diseases	[144]
^{64}Cu	DOTA-HB (hexadecyl-benzoate)	adipose-derived stem cells (ADSCs)	PET of transplanted stem cell	***in vitro & in vivo*** in rat heart with intramuscularly transplanted ADSCs	[145]
^{64}Cu	NO2A-(X)-BBN(7−14)NH_2	bombesin (BBN) receptor	PET of human PC	***in vitro & in vivo*** in prostate tumor xenografted mouse models	[146]
^{64}Cu	NODAGA-galacto-BBN	Gastrin-releasing peptide receptor (GRPR)	PET of GRPR-positive tumors	***in vitro & in vivo*** in PC3 tumor-bearing nude mice	[147]
^{64}Cu	NO2A-RGD-Glu-6-Ahx-BBN(7−14)NH_2	GRPR; BBN(7−14)NH_2	microPET	***in vitro & in vivo*** in PC-3 tumor-bearing rodent models	[148]
^{64}Cu	NOTA and BBN derivatives	GRPR over-expressed PC-3	PET imaging	***in vitro & in vivo*** in Wistar rats and nu/nu mice bearing the human prostate tumor PC-3	[149]
^{64}Cu-NOTA/(DOTA)-GGNle-CycMSH$_{hex}$		melanocortin-1 (MC1) receptor	PET/CT of melanoma	***in vitro & in vivo*** in B16/F1 melanoma-bearing mice	[150]
^{64}Cu	NOTA-bevacizumab	angiogenic factor VEGF	microPET/CT and therapy monitoring	***in vitro & in vivo*** in 786-O renal carcinoma xenografts	[151]
^{64}Cu	*p*-NH_2-Bn-NOTA-anti-CD99 antibody	CD99 positive tumors (Ewing sarcoma)	PET of tumors and metastases	***in vitro & in vivo*** in mice with subcutaneous Ewing sarcoma and metastatic sites	[152]
^{64}Cu	MANOTA NODAGA and DOTAGA - Fab-trastuzumab	HER2/neu receptor positive tumors	PET of tumors	***in vitro & in vivo*** breast cancer cells in xenografted mice	[67]
^{64}Cu	NE3TA-PEG4-LLP2A and NE3TA-cetuximab	VLA-4-overexpressed-tumor	PET/CT imaging	***in vitro & in vivo*** in mice bearing VLA-4 positive B16F10 mouse melanoma cells	[153]
^{64}Cu	H40−P(LG-Hyd-DOX)-*b*-PEG-OCH_3/cRGD-NOTA	$\alpha_v\beta_3$ integrin targeting	PET and cancer theranostics	***in vitro & in vivo & ex vivo*** in U87MG tumor-bearing mice	[154]
^{64}Cu	CB-TE2A-c(RGDyK)	$\alpha_v\beta_3$ integrin targeting	PET imaging of osteoclasts	***in vitro & in vivo & ex vivo*** from bone marrow macrophages	[155]
^{64}Cu	CB-TE1A1P−Y3-TATE	SSTR positive tumors	PET/CT imaging	***in vitro & in vivo*** in rats with AR42J pancreatic tumor	[156]
^{64}Cu	CB-TE1A1P-DBCO-Y3-TATE	SSTR2	PET/CT imaging	***in vitro & in vivo*** in SSTR2-transfected HCT116 tumor-bearing female nu/nu mice	[157]
^{64}Cu	CB-TE2A-YPSMA-1 or Bavituximab	PSMA and phosphatidylserine antibody (Bavituximab)	PET imaging	***in vitro & in vivo*** in mouse xenograft model, demonstrating a click-chemistry strategy	[158]
^{64}Cu	CB-TE1A1P-LLP2A	VLA-4 (very late antigen-4)	PET/CT of multiple myeloma	***in vitro & in vivo*** in 5TGM1 tumor bearing syngeneic KaLwRij mice	[159]
^{64}Cu	CB-TE1A1P and CB-TE1K1P	EGFR and cetuximab	PET/CT colorectal cancer	***in vitro & in vivo*** in HCT116 tumor-bearing mice	[160]
^{64}Cu	PCB-TE2P and PCB-TE1A1P		PET imaging	***in vitro & in vivo*** biodistribution in rats and mice	[161,162]
^{64}Cu	CH_3-(p-NCS-Ph)-Sar-trastuzumab	HER2-positive cancer	PET imaging	***in vitro & in vivo*** in mice bearing BT-474 human breast carcinoma xenografts	[163]
^{64}Cu	Sar conjugated to antibody fragment (scFv$_{anti-LIBS}$)	ligand-induced binding sites (LIBS) on glycoprotein receptor GPIIb/IIIa	PET diagnostics of activated platelets	***in vitro & in vivo*** in mice model of carotid artery thrombosis	[164]
^{64}Cu	MeCOSar-scFv$_{anti-GPIIb/IIIa}$	GPIIb/IIIa	PET of acute thrombosis	***in vitro & in vivo*** in mice model of injured and noninjured vessel	[165]
^{64}Cu	MeCOSar-scFv$_{anti-LIBS}$	LIBS on GPIIb/IIIa	PET of activated platelets	***in vitro & in vivo*** in mice model of minimal cardiac ischemia	[166]
^{64}Cu	Sar and MeCOSar-PEGx-BN conjugates	GRPR	PET	***in vitro & in vivo*** biodistribution in mice	[167]
^{64}Cu	SarAr-BN (7−14) conjugate	GRPR	PET of prostate cancer	***in vitro & in vivo*** in PC-3 cells and xenografted mice	[168]
^{64}Cu	Sar-TATE	somatostatin receptor 2	PET	***in vitro & in vivo*** biodistribution in mice	[169]
^{64}Cu	Sar - c(RGDyC)	$\alpha_v\beta_3$ integrin targeting	PET	***in vitro & in vivo*** in U87MG glioblastoma xenograft model	[170]
^{67}Cu	2IT-BAT-Lym-1;	Lym-1	Radioimmu-notherapy for lymphoma	***in vitro & in vivo*** in mice implanted with human Burkitt's lymphoma (Raji)	[171]
^{67}Cu	2IT-BAT-Lym-1	Lym-1	Radioimmu-notherapy for lymphoma	**Clinical studies** on 3 patients with non-Hodgkin's lymphoma (NHL) stage IVB, resistant to standard therapy; 4 patients with B-lymphocytic NHL; 10 lymphoma patients	[172] [173] [174]
^{67}Cu	[^{67}Cu]$CuCl_2$	major organs for copper metabolism	radiotherapy	***in vitro & in vivo*** in colorectal tumor-bearing mice	[175]
^{67}Cu	cyclam-RAFT-c(RGDfK)$_4$	$\alpha_v\beta_3$ integrin, transmembrane receptor	$\alpha_v\beta_3$ integrin-targeted internal radiotherapy	***in vitro & in vivo*** in mice with subcutaneous $\alpha_v\beta_3$ positive U87MG-glioblastoma xenografts	[176]

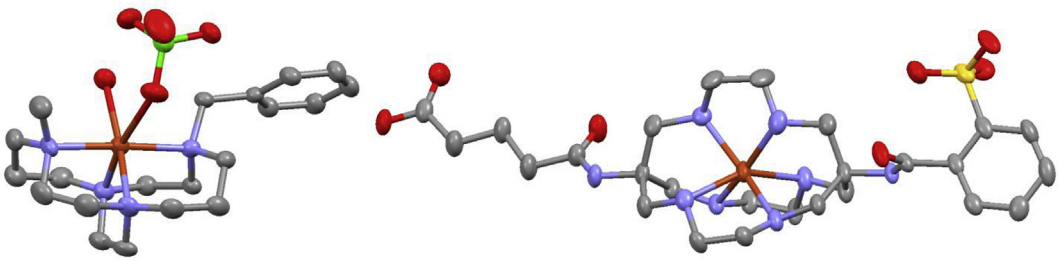

Fig. 2. Crystal structures of two Cu(II) complexes, namely Cu(II) complex with unsymmetrically functionalized CB-TE2A (left [54]) and a neutral zwitterionic Cu(II) complex of Sarcophagine derivative (right [77]) Hydrogen atoms are omitted for clarity.

pyridyl N- atom, has been demonstrated on some pentadentate cross-bridged cyclam derivatives (pycup) with different pendant arms. While the type of the latter was not crucial, more detail studies of the carboxylic derivative proved its good kinetic inertness toward ^{64}Cu decomplexation and relatively favorable radiolabeling conditions (15 min at 70 °C, or 30 min at 60 °C). Biodistribution studies in mice revealed low residual activity in kidney, liver, and blood pool with predominant renal clearance of the Cu-pycup complexes. Furthermore, the carboxylic derivative has been conjugated to a fibrin-targeting peptide to demonstrate its successful use for ^{64}Cu-PET imaging of arterial thrombosis in a rat model [61].

Unarguably, the requirements for ideal bifunctional chelator for copper radiopharmaceuticals are multifaceted and very challenging. There is increasing amount of evidences, however, on the nearly excellent efficiency of the smaller size triazamacrocyclic NOTA chelators and the macrobicyclic sarcophagine cages (Sar), as reported by Cooper et al. [47] and in many other comparative studies. The NOTA and Sar bifunctional chelators conjugated with the anti-CD20 antibody rituximab showed significant advantages over the macrocyclic analogues DOTA, DO3A, and PCTA, by providing rapid radiolabeling at room temperature and under dilute conditions, as well as exceptionally high resistance to transchelation *in vivo*. Despite the many examples of successful application of C-linked NOTA BFCs as ^{64}Cu-radiopharmaceuticals [45,62–64], new derivatives of NOTA, with at least one pendant carboxylic group modified, have continuously been studied [44,64–66] and some are depicted in Fig. 1. Recently, Moreau et al. demonstrated the superior ^{64}Cu-labeling ability of MANOTA derivative (that is methyl amino triazacyclononane triacetic acid) in comparison with NODAGA and DOTAGA chelators – all bearing a p-benzyl isothiocyanate group conjugated to Fab-trastuzumab for targeting the HER2/neu receptor of breast cancer cells in xenografted mice [67]. The demonstrated favorable pharmacokinetic profiles for most of NOTA, NO2A, and NE3TA linked bioconjugates justify the intense research interest in this class of chelators as potentially useful for diagnostic and/or therapeutic applications (Table 2).

The macrobicyclic sarcophagines, developed by Sargeson [68–70], have later been utilized by the same authors as chelators for copper radionuclides, conveniently conjugated to fragmented and whole antibodies or even nanoparticles, to prove their potent applicability in high-precision PET imaging [71–73]. The major advantages of Sar family include the following characteristics – they complex [^{64}Cu]Cu^{2+} rapidly, quantitatively and essentially irreversibly at pH 5 and RT for < 5 min; modifications are usually easy and allow ready conjugation to proteins without impairing the coordination of the [^{64}Cu]Cu^{2+}; exceptionally high *in vivo* stability and kinetic inertness to transchelation even in presence of 0.1 M EDTA. All these favorable properties of sarcophagine cages have ensured the excellent performance of ^{64}Cu-Sar-bioconjugates as PET tracers in animal studies [74,75], and initiated many new synthetic [76] and biomolecular modifications [77,78].

Structural functionalizations of the discussed chelators are needed steps in the preparation of BFCs introducing suitable sites for fast and easy (bio)conjugation. In some cases the structural modifications can affect the chelating unit, or can be placed at a more distant part of the molecule. In both cases, however, the biodistribution of the carried radio-copper changes, either by modulating the stability of the formed Cu(II) complexes (i.e. its readiness for transchelation) or by changing the charge, lipophilicity/hydrophilicity of the complex. Selected crystal structures of copper complexes of structural analogues of two of the best chelators for Cu(II) – CB-TE2A and Sarcophagine – depict these two cases (Fig. 2). The unsymmetrical modification of CB-TE2A with two non-coordinating side arms, as a needed synthetic step for further functionalization [54], turns CB-TE2A into a four-dentate ligand that coordinates Cu(II) in the way presented in Fig. 2 (left). The Sarchelator depicted in Fig. 2 (right) is modified with carboxylate and sulphonate groups far from the donor atoms in the bicyclic unit, and thereby only the overall charge of the formed complex is altered; a neutral zwitterionic Cu(II) complex is formed [77]. Comparative study on tissue uptake of antibody fragment labeled with ^{64}Cu through SarAr and other chelators of different total charge indicated that reducing the positive charge on the complex results in 6-fold decrease of the kidney uptake of the ^{64}Cu-labeled antibody [77].

Once the best chelator and the biomolecular vector have been selected for a predefined medical purpose, the conjugation of these two fragments is a matter of additional concerns. Depending on the reaction conditions required for both the bioconjugation and the radionuclide chelation, two different approaches can be used – prelabeling and post-labeling. In the prelabeling approach the radionuclide is complexed by the chelator before it is conjugated to the biovector. This strategy is required when the chelation proceeds under harsher conditions, which can damage the biomolecular vector, and the bioconjugation is easy and non-detrimental for the radiometal complex. Conversely, when the bioconjugation step is more intricate and requires further purifications, the post-labeling approach is more appropriate, since the rapid radiolabeling of the chelator is performed after it is conjugated to the biovector. This approach is required when a short-lived radioisotope has to be utilized. Therefore, the reaction conditions for the bioconjugation step are equally important to the chelation kinetics and the stability of the radiocomplex.

The highly specific, robust and efficient “click reactions” give strong benefits in the strategies for design and development of advanced target-specific radiopharmaceuticals [79]. Among the well-established “click reactions” – Cu(I)-catalyzed azide–alkyne cycloaddition (CuAAC) reactions, the copper-free strain-promoted azide–alkyne cycloaddition (SPAAC), inverse electron demand Diels-Alder reaction (IEDDA), and the Staudinger ligation – the

CuAAC is usually avoided or only rarely used in constructing copper radiopharmaceuticals [80]. The other three types of reactions meet the major requirement imposed to *bioorthogonal* "click reactions" – to be inert within biological systems [81]. The principles of "click chemistry" proved useful not only for radiolabeling reactions employing a set of "clickable" groups, but also for site-specific bioconjugation of peptides and antibodies, and more recently, for *in vivo* pretargeting. The clickable groups used for copper radiopharmaceuticals have evolved from N-hydroxysuccinimidyl (NHS) esters and maleimides, used for coupling with the lysines and cysteines from peptides [82], to analogues of cyclic alkyne dibenzocyclooctyne (DBCO) for conjugation with an azide (SPAAC reaction) [83], and tetrazines (Tz) to be clicked with the most commonly used dienophiles – *trans*-cyclooctene (TCO) [84–88] and norbornene (NB) [89] in the IEDDA reaction. The principles of the SPAAC and IEDDA reactions are depicted in Fig. 3 as they are the preferred methods for bioorthogonal modifications of copper-based radiopharmaceuticals. Indeed, these methods have been utilized in the synthesis of most of the copper radiopharmaceuticals exemplified in this and the following sections.

The pretargeting approach is the most advanced way to limit the risks of excess radiotoxicity delivered by radioimmunoconjugates that results from the long blood circulation of the MAbs and their slow accumulation at the target organs with slow subsequent clearance [90]. This approach utilizes either specific non-covalent interactions or covalent bond formations based on bioorthogonal "click reactions" that occur in the patients' body between the preadministered, and already tumor bound, antibody and the radiolabeled small molecule (hapten) that is administered in a second step. After 30 years of elaboration of the pretargeting strategy, significant amount of information from preclinical and clinical trials is already acquired and the achieved progress have recently been reviewed highlighting the advantages and limitations of this strategy [91,92]. The (strept)avidin-biotin recognition system, although regarded as a gold standard for the two-step pretargeting approach, still poses unresolved problems related to immunogenicity caused by the repeated biotin administration. Data from phase II clinical trial on the use of a three-step pretargeting system – [^{90}Y]Y-DOTA-biotin and NR-LU-10 antibody/streptavidin – to treat patients with metastatic colon cancer gave disappointing results related to inability to deliver sufficiently high doses to tumor due to dose-limiting normal tissue toxicity, hematological and non-hematological toxicities [93]. Despite these limitations, the (strept)avidin-biotin system has proved the principles of using specific non-covalent interactions in pretargeting strategy. The use of bispecific antibodies, which bind tumor-specific antigen and radiolabeled hapten administered in a second step, is steadily developing and has demonstrated improved targeting efficiency in preclinical models. Recent results from phase I clinical trials on the use of bispecific antibody (TF2) for radioimaging and radioimmunotherapy of colorectal cancer in 21 patients concluded that this system achieves highly specific and rapid tumor targeting [94]. For radiolableing with ^{111}In/^{177}Lu a DOTA chelator, attached to a peptide bearing histamine-succinylglycine (HSG) hapten, has been used. Many more examples demonstrating the advancements in the design and application of bispecific antibodies have recently been reviewed [95].

The chemical modification of antibodies is the major synthetic challenge to be overcome for broader utilization of the pretargeting strategy. Site-specific conjugation with antibodies is recognized as superior to the nonspecific chemical conjugation as it provides better homogeneity, reproducibility, and higher possibility to preserve the biological function of the MAb [96]. Enzyme-mediated modifications using bacterial transglutaminases, Sortase A (SrtA)

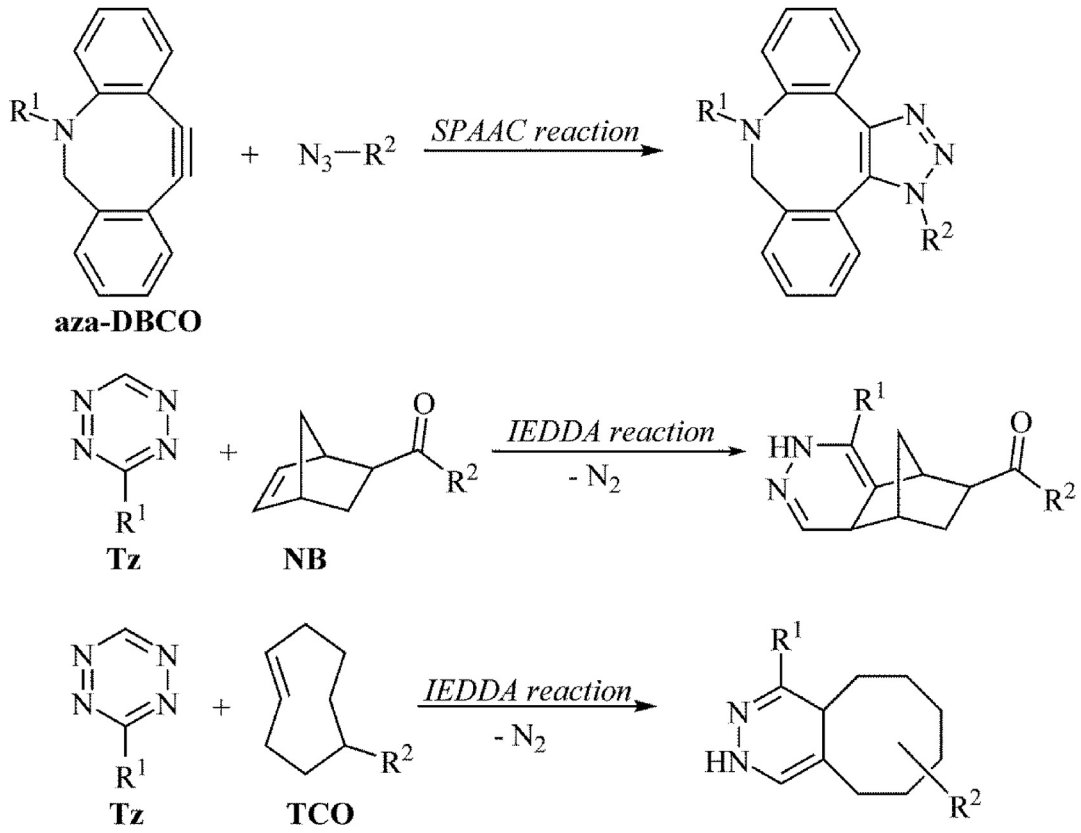

Fig. 3. Click reactions most commonly used for the synthesis of target-specific bifunctional chelators for copper(II).

or other enzymes proved very successful for protein engineering and antibody modification [97]. Thereby, the enzyme-mediated site-specific conjugation of bioorthogonal clickable groups to biomolecules can provide versatile pathways for further multistep modifications [4]. The use of bioorthogonal click chemistry for covalent bonding in the pretargeting strategy is rapidly advancing. An example to mention is a pretargeting achieved by supramolecular system used as vector that is based on nanoparticles (NPs) encapsulating the reactive bioorthogonal *trans*-cyclooctene (TCO) – to form a TCO⊂SNPs complex – and a DOTA-linked tetrazine (Tz) suitable for radiolabeling with ^{64}Cu and for bioorthogonal IEDDA click reaction [87]. Comparison of the microPET/CT images of mouse models xenografted with U87 glioblastoma cells and treated with the designed supramolecular system (TCO⊂SNPs), or with its components separately, indicated an excellent specificity in the tumor localization by the pretargeted system of TCO⊂SNPs complex and [^{64}Cu]Cu-DOTA-Tz (Fig. 4, a) that is governed by the EPR effect [87].

4. Current state of medical uses of copper radiopharmaceuticals

Despite the available alternatives for producing the biomedical radionuclides of copper, their cost remains so far a limiting factor. Nevertheless, intense research is undergoing for the development and optimization of the radionuclide production methods as well as the design of novel highly specific radiopharmaceuticals. The numerous investigations of copper radiopharmaceuticals, however, are mostly at the stage of preclinical studies; only 15 clinical trials are listed in the ClinicalTrials.gov database by the end of 2017. Most of these studies (12) are related to ^{64}Cu-labeled PET tracers [98], and only three trial studies have been initiated on ^{62}Cu candidates [99]. Nevertheless, the achieved advancement in the design and evaluation of various copper chelators, linking and targeting units, as well as the emerging pretargeting and nanodelivery strategies give the hope that the copper radiopharmaceuticals will become powerful theranostic tools in the near future. The studies verifying the applicability of ^{60,62,64}Cu nuclides for imaging purposes usually compare their performance with the FDA-approved agent [^{18}F] fluorodeoxyglucose (FDG), whereas the therapeutic potential of ^{64}Cu and ^{67}Cu nuclides is often compared with that of the beta emitters ^{131}I or ^{90}Y – established radioimmunotherapeutics. The available data from clinical and recent preclinical studies on all five copper radioisotopes and the corresponding radiopharmaceuticals are summarized in Table 2.

The use of ^{60}Cu-labeled ATSM for imaging hypoxic tissues, relevant with several types of cancer, has been in clinical trials and some results on the applicability of PET to patients with non-small-cell lung cancer (NSCLC) [100] or cervical cancer have been reported [101,102]. Data from clinical tests, performed in Japan, on the

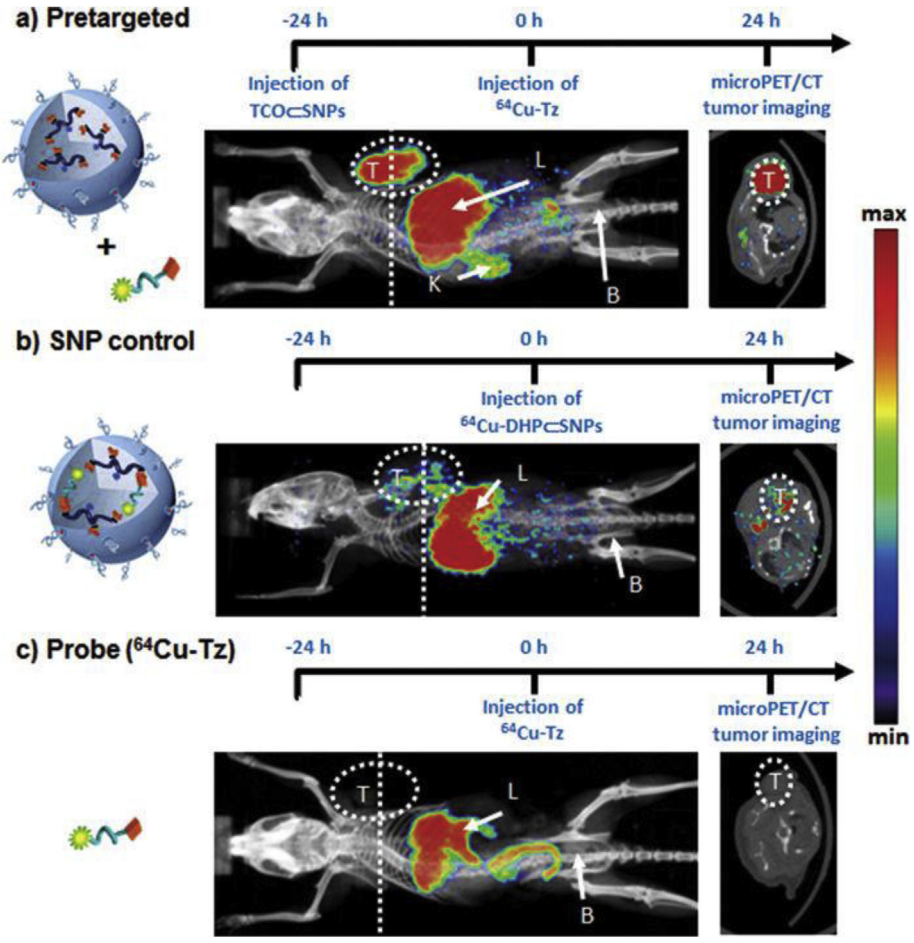

Fig. 4. Timeline of the injection protocol employed for (a) pretargeted, (b) SNP control ([^{64}Cu]Cu-DHP⊂SNPs), and (c) free radiolabeled reporter ([^{64}Cu]Cu-Tz) studies. Representative *in vivo* microPET/CT images of the mice (n = 4/group) subjected to the three studies at 24 h p.i. Labels T, L, K, and B refer to the tumor, liver, kidney, and bladder, respectively. Dashed lines correspond to the transverse cross-section through the center of each tumor mass, whose image is shown in the right panel. Adapted with permission from ref. 87, copyright American Chemical Society.

use of ^{62}Cu-PET evidenced that [^{62}Cu]Cu(ATSM)-PET can be useful for disease prognosis of patients with head-and-neck cancer (HNC) [103,104] as well as for predicting malignant hypoxic tissues in patients with glioma [105,106]. The readily available production method of the ^{62}Cu isotope (from ^{62}Zn/^{62}Cu generators [12]) overcomes the limitation of its very short half-life, and had advanced to automated synthesis of [^{62}Cu]Cu(PTSM) to be used in clinical PET [107] and for imaging cardiac perfusion abnormalities [108]. Combination of [^{62}Cu]Cu(ATSM)- and [^{62}Cu]Cu(PTSM)- PET, augmented with FDG-PET/CT technique or proteomic analyses, can provide information on perfusion and hypoxia as well as tumor anatomy and metabolism [109,110], thereby presenting alternatives to invasive biopsies.

As mentioned before, the areas of radiopharmaceutical applications are most extensively studied for ^{64}Cu isotope due to its favorable nuclear properties, which make make it suitable for both diagnostic imaging and therapy. The biological basis of medical application of [^{64}Cu]Cu^{2+} ions and all reported data related to the way of the radionuclide production has recently been reviewed by Chakravarty et al. [111]. Preliminary results from clinical studies on the use of radiolabeled [^{64}Cu]$CuCl_2$ demonstrated its applicability for PET/CT imaging of patients with prostate cancer [112]. Moreover, the [^{64}Cu]$CuCl_2$ proved useful as a diagnostic tracer for PET imaging of brain tumors in 19 patients with cerebral tumors [113]. The theranostic application of [^{64}Cu]$CuCl_2$ has been suggested by the results from preclinical studies on successful treatment and PET visualization of two types of melanoma (B16F10 and A375 M) that overexpress CTR1 ensuring the high affinity to copper ions [114]. Earlier clinical studies in patients with cervical cancer concluded that the [^{64}Cu]Cu(ATSM) provides PET images of better quality than [^{60}Cu]Cu(ATSM) [115]; and more recent clinical data demonstrated that [^{64}Cu]Cu(ATSM) PET/CT can provide semiquantitative and quantitative parameters in patients with NSCLC for reliable prognosis of the disease outcome [116]. The longer half-life of ^{64}Cu (~12.8 h) offers a larger variety of radiolabeling strategies – from peptide labeling to pretargeting approaches using bifunctional chelators and click chemistry. Clinical studies on the use of ^{64}Cu-labeled TP3805, which is a PACAP analogue with a C-terminal diaminodithiol (N2S2) chelator, for PET/CT imaging of patients with breast [117] or prostate cancer [118] indicated that [^{64}Cu]Cu-TP3805 is worthy of distinguishing malignant lesions from benign tissues and can be used as noninvasive alternative to unnecessary biopsies. Suitably modified thiosemicarbazones that bind amyloid-β plaques have been used to chelate ^{64}Cu for PET imaging of Alzheimer's diseases in post-mortem human brain tissues as well as in wild-type mice [119].

The high potential for selective targeting by means of macrocyclic bifunctional chelators has been extensively used for imaging and therapeutic purposes based on ^{64}Cu isotope. The cyclam derivative TETA is the tetraazamacrocyclic chelator most commonly used for Cu(II). Clinical data on some TETA and somatostatin-receptor targeting conjugates, including octreotide (OC) or Tyr3-octreotate (Y3-TATE), demonstrated the power of [^{64}Cu]Cu-TETA-OC PET imaging in patients with neuroendocrine tumors [120]. In earlier preclinical studies, these substances have successfully been used for targeted radiotherapy in rats bearing somatostatin receptor-positive tumors [121,122] and identified the bladder or liver as dose-limiting organs. TETA has also proved useful for labeling various bombesin (BN) peptides with ^{64}Cu and ^{67}Cu and has been exploited for *in vivo* PET imaging and targeted radiotherapy of BN receptor-positive tumors, such as PC-3 tumors [123].

The tetraazamacrocyclic chelator DOTA, although forming copper complexes of lower *in vivo* stability than TETA, has also been extensively used for ^{64}Cu-labeling in numerous biological studies, which can be explained with the available FDA-approved DOTA chelators for diagnostic imaging or radiotherapy with various metal ions – Gd(III), [^{68}Ga]Ga^{3+}, [^{111}In]In^{3+}. Initial preclinical studies showed that successful PET imaging of angiogenesis can be achieved in various tumor models by targeting the endothelial growth factor receptors (EGFR) [124] or $\alpha_v\beta_3$ integrins [125,126] with [^{64}Cu]Cu-DOTA labeled specific peptide fragments. Many more examples appeared in the last five years on the use of peptide fragments as biomolecular vectors for targeting [^{64}Cu]Cu-DOTA to various tumor-associated receptors [127–130]. Deng et al. developed a dual-modality probe [^{64}Cu]Cu-DOTA-NT-Cy5.5 for imaging of neurotensin receptors expression *in vivo* with both PET and fluorescence. This was achieved by chemical modification of neurotensin analogue (Cys-NT) with the Cy5.5 dye and DOTA-NHS. The authors claim that probe stability in PBS was good for up to 6 h post incubation but additional improvements are still needed to overcome the higher liver uptake seen in PET images than in fluorescence images [129]. More advanced approaches incorporated ^{64}Cu-complexes of DOTA in suitably modified purpose-specific liposomes to be used for both imaging and therapy of angiogenesis [131] or neuroendocrine tumors (NETs) [132]. In the former case tetraiodothyroacetic acid (tetrac) was conjugated to the liposomes leading to 10 times higher uptake in human aortic endothelial cells (HAEC) than the [^{64}Cu]Cu-DOTA-liposomes, whereas the accumulation of [^{64}Cu]Cu-DOTA-PEGylated liposomes in the NETs was not affected by conjugation with TATE. Both types of liposomes exhibited significantly higher tumor uptake than the free ^{64}Cu-DOTA-labeled TATE peptide. Currently, the use of monoclonal antibodies for highly specific targeting of DOTA-chelated [^{64}Cu]Cu^{2+} becomes preferred method for tumors [133–136], lymphomas [137,138] and metastases imaging [139]. Wang et al. developed a^{64}Cu-labeled probe for PET imaging of BXPC3 pancreatic tumors overexpressing GRP78 receptor by utilizing the anti-GRP78 monoclonal antibody MAb159. Binding activity assay showed that [^{64}Cu]Cu-DOTA-MAb159 preserved 85% of the GRP78-binding activity of the unmodified monoclonal antibody [135]. Schjoeth-Eskesen et al. optimized the labeling of trastuzumab with ^{64}Cu to be used as HER2-positive breast cancer probe. The ^{64}Cu-labeling of trastuzumab mediated by NODAGA as chelator was not as high as for DOTA analogue. Both tracers showed high tumor uptake, as evidenced by small-animal PET/CT imaging of mice with HER2 expressing tumors, and exhibited high *in vivo* stability proved by blood samples analyses [136]. The numerous applications of ^{64}Cu-DOTA-labeled MAbs range from synergistic combination of cancer radioimmunotherapy with chemotherapy [140] to imaging of myocardial infarction [141], or atherosclerotic plaques [142] and Alzheimer's disease associated Aβ plaques [143]. Interesting cases have been presented on the use of nanoparticles (NPs) conjugated with [^{64}Cu]Cu-DOTA and anti-ICAM antibody to target intercellular adhesion molecule 1 (ICAM-1) for targeted therapy of acute and chronic respiratory diseases, which was clearly visualized by small-animal PET [144]. More recently, [^{64}Cu]Cu-DOTA-HB has been conjugated to adipose-derived stem cells (ADSCs) and used as PET radiotracer for imaging of stem cells intramuscularly transplanted in normal rat heart [145].

To overcome the major challenges of ^{64}Cu-labeling through TETA and DOTA chelators – as unfavorable labeling conditions and *in vivo* transchelation – a smaller size triazamacrocycle NOTA has been developed and used in a series of preclinical studies. Different NOTA derivatives have been conjugated with bombesin peptide and successfully used for *in vivo* ^{64}Cu-PET imaging of prostates cancer [146–149], whereas NOTA-radiolabeled cyclic peptides proved efficient for targeting melanoma in mice and its successful imaging and therapy [150]. PET/CT imaging of high quality have been achieved with ^{64}Cu-NOTA-labeled antibodies and demonstrated the possibility to use them for imaging and monitoring

diseases therapy including some micrometastasis [151,152]. Recently, Moreau et al. synthesized a new bifunctional derivative of NOTA, MANOTA, conjugated to Fab-trastuzumab through a p-benzyl isothiocyanate group and demonstrated its better ^{64}Cu-labeling ability than NODAGA and DOTAGA analogues that resulted in improved imaging of breast cancer cells xenografted in mice [67]. Gai et al. synthesized a new bifunctional derivative of NOTA, the NE3TA (Fig. 1), containing propyl chain to reduce the potential steric hindrance during the chelation and showed higher selectivity to form stable complexes with Cu(II) over Fe(III). The peptidomimetic conjugates [^{64}Cu]Cu-NE3TA-PEG4-LLP2A and [^{64}Cu]Cu-NOTA-PEG4-LLP2A have been compared with the corresponding cetuximab antibody conjugates and showed high potential for PET/CT imaging of B16F10 melanoma xenografts in mice [153]. Another approach used multifunctional hybrid system for theranostic application based on a micelle-forming hyperbranched block copolymer conjugated to cyclic RGD peptide, ^{64}Cu-labeled NOTA and the anticancer drug - doxorubicin (DOX) [154]. The formed cRGD-conjugated unimolecular micelles (H40-DOX-cRGD) exhibited high cellular uptake in U87MG human glioblastoma cells, and demonstrated good *in vivo* synergy between their tumor-targeting abilities and the pH-controlled drug release in mice xenografts. Furthermore, the observed therapeutic effects have been coupled with concomitant PET imaging, raising high hopes of building successful cancer-targeted theranostics.

In vivo studies have demonstrated that [^{64}Cu]Cu-CB-TE2A conjugated to a cyclic peptide c(RGDyK) or a somatostatin analogue, Tyr3-octreotate (Y3-TATE), can be used to identify osteolytic bone metastasis and inflammatory osteolysis [155], and somatostatin-receptor positive neuroendocrine tumors [156,157]. Preclinical PET/CT imaging has been demonstrated using [^{64}Cu]Cu-CB-TE2A labeled antibodies in a mouse xenograft model [158]. In this study Kumar et al. used click-chemistry strategy to link the [^{64}Cu]Cu-CB-TE2A moiety with two MAbs via the tetrazine-norbornene mediated click reaction. Similarly, the CB-TE1A1P analogue has been utilized to label antibodies, through advanced click-chemistry strategies, and proved useful for imaging multiple myeloma tumors [159] or EGFR-positive tumors [160]. Propylene cross-bridged macrocyclic chelators (PCB-TE2P and PCB-TE1A1P) have been synthesized and tested for Cu(II)-complexation, Cu(II)-complex stability, ^{64}Cu-radiolabeling, and *in vivo* behavior in comparison with other bicyclic chelators [161,162]. The propylene-cross-bridged cyclam chelator PCB-TE1A1P, reported by Dale et al., bears hybrid acetate/phosphonate pendant groups that ensured a very high stability of its Cu(II) complex remaining intact for 8 days at 90 °C in 12 M HCl [162]. The biodistribution and *in vivo* stability profiles of [^{64}Cu]Cu-PCB-TE1A1P confirmed that the radioactive complex remains stable under physiological conditions and clears rapidly from the body.

The most promising copper chelators are the macrobicyclic cages, known as “sarcophagine” (Sar), which allow fast labeling at room temperature (~5 min) with high radiochemical purity (>95%) and remarkable kinetic inertness of the resulting Cu complex. This was demonstrated in many *in vivo* studies on biodistribution and PET imaging employing [^{64}Cu]Cu-Sarcophagine conjugated to antibodies [163–166] or peptides [167–170]. Targeting gastrin-releasing peptide receptor (GRPR) by ^{64}Cu-Sar-labeled bombesin [168] or bombesin receptor antagonist [167] proved successful in

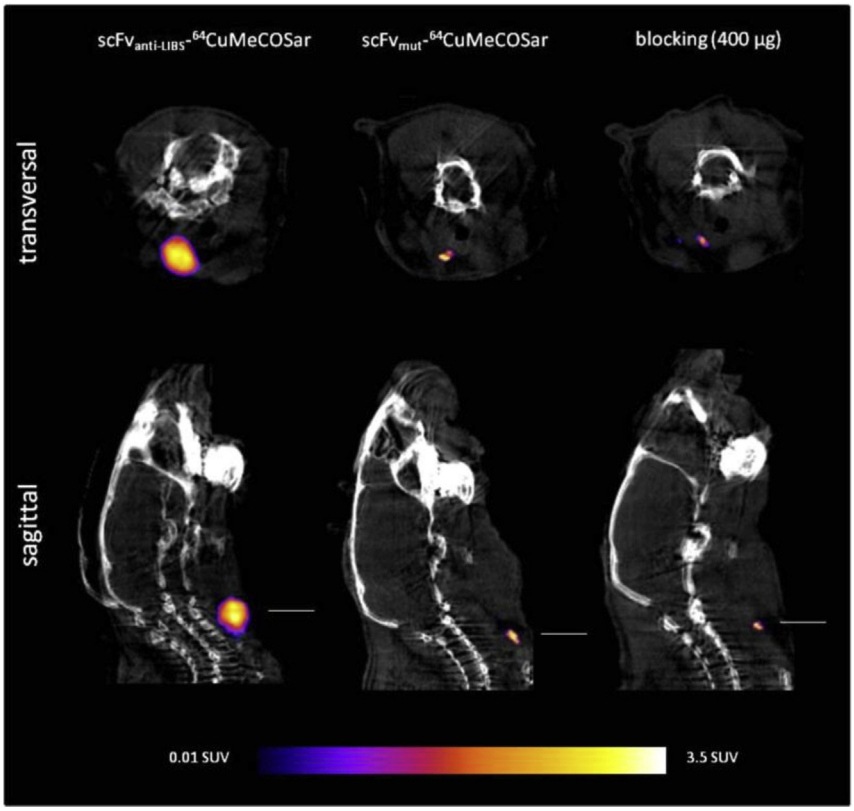

Fig. 5. Serial small-animal PET images of an *in vivo* model of mouse carotid artery thrombosis 60 min after injection of the radiotracer. Comparison of representative transverse and sagittal PET images of scFv$_{anti-LIBS}$-[^{64}Cu]Cu-MeCOSar and scFv$_{mut}$-[^{64}Cu]Cu-MeCOSar and a blocking experiment by injecting scFv$_{anti-LIBS}$ 30 min before injection of scFv$_{anti-LIBS}$-[^{64}Cu]Cu-MeCOSar is shown (n = 6). The color scale for all PET image data shows radiotracer uptake in units of standard uptake value (SUV), with white corresponding to the highest activity and blue to the lowest activity. Adapted with permission from ref. 165, copyright American Chemical Society. (For interpretation of the references to color in this figure legend, the reader is referred to the Web version of this article.)

PET imaging of prostate cancer. Interestingly, in some studies on single-chain antibodies labeled by ^{64}Cu-Sar derivatives, demonstrated efficient PET imaging of activated platelets that is related to artery thrombosis [165] and cardiac ischemia [166]. Images of small-animal PET of mouse carotid artery thrombosis demonstrate very high selectivity of the ^{64}Cu-MeCOSar-labeled immunoconjugate ($ScFv_{anti\text{-}LIBS}$-[^{64}Cu]Cu-MeCOSar) in targeting activated platelet 1 h after injection, as depicted in Fig. 5. The attempts for labeling an analogous antibody using DOTA chelator resulted in very low specific activity of the corresponding constructs, most probably due to the harsher labeling conditions that are required for DOTA.

Details on the biological targets and area of radiopharmaceutical applications are listed in Table 2, which summarizes the current state of the medical applications of copper radionuclides with focus on the last 5 years.

Radioimmunotherapy has been in clinical use for lymphoma treatment with ^{131}I-radiolabeled Lym-1, a mouse anti-lymphoma monoclonal antibody. This initiated several preclinical studies on the efficacy of ^{67}Cu-radiolabeled Lym-1, namely 2IT-BAT-Lym-1 where BAT is conjugated to Lym-1 via 2-iminothiolane (2IT), to treat Burkitt's lymphoma (Raji) tumors in mice [171]. Clinical studies on the therapeutic index in patients with Ann Arbor stage IVB NHL resistant to standard therapy [172], and lymphoma patients [173,174] have also been started. The results concluded that in many aspects the [^{67}Cu]Cu-2IT-BAT-Lym-1 is superior to [^{131}I]I-Lym-1 for providing a remarkably high therapeutic index. The successful application of different ^{67}Cu-labeled antibodies for radioimmunotherapy have been compared with other radioisotopes and summarized by Novak-Hofer and Schubiger, who also indicated that the limiting factor for more intense clinical trials in this direction is the availability of ^{67}Cu radionuclide [21]. Therefore, different methods for ^{67}Cu radionuclide production, and their biological applicability, have been investigated continuously. A very recent study from 2017 evaluated the biodistribution of [^{67}Cu]$CuCl_2$ (with ^{67}Cu produced by the ^{68}Zn(n,n′pd)^{67}Cu reaction) in colorectal tumor bearing mice. High uptake of ^{67}Cu was observed in the tumor but also in the liver and kidney, similarly to what is observed for [^{64}Cu]$CuCl_2$, as they are organs strongly involved in the copper metabolism [175]. In another study from 2017, the ^{67}Cu produced from ^{64}Ni(α, p)^{67}Cu reaction was used for radiolabeling of a tetrameric cyclic Arg-Gly-Asp (cRGD) peptide by cyclam-RAFT for targeting angiogenesis and metastasis. The administration of a single dose of [^{67}Cu]Cu-cyclam-RAFT-c(RGDfK)$_4$ resulted in significant delay of the tumor growth indicating its high therapeutic potential for $\alpha_v\beta_3$ integrin-targeted radiotherapy [176].

5. New trends and requirements for theranostic applications of copper radionuclides

The theranostic strategies aim to monitor targeted delivery of drugs by integrating the diagnosis and treatment modalities in one pharmaceutical formulation and at the same dosage range. Therefore, a theranostic agent must contain a therapeutic drug, targeting biomolecular vector and signal emitter, all of which are usually loaded into or bound to a delivery platform. To fulfill all these tasks nanotheranostic materials (such as mesoporous, metallic, or magnetic nanoparticles (NPs), liposomes, micelles, dendrimers, biopolymers etc.) have been broadly employed as delivery platforms capable of versatile modifications and covalent or non-covalent attachment of all needed constituents [177,178]. Recently Lovell et al. summarized the achievements in the development of advanced theranostic materials that meet the requirements for their diagnostic and therapeutic applications, so that the improved disease detection and enhanced chemotherapeutic treatments be appropriate for clinical translations [179]. The use of nanoparticles for PET imaging had already expanded to dual-labeled materials [180], which can be used as optical/PET or MRI/PET tracers for whole-body diagnostics and/or intraoperative image-guided tumor resection. Besides, antibody- and peptide-based multimodal imaging agents may also induce antibody-dependent cell-mediated cytotoxicity [181], providing additional functionality. Incorporation of a therapeutic component into model nanotheranostics has been achieved using the anticancer drug doxorubicin (DOX) and established techniques for covalent conjugation with polymers or physical encapsulation by unimolecular micelles. In the former case doxorubicin has been conjugated with amphiphilic block copolymer to form poly(L-glutamate-hydrazone-doxorubicin) arms further decorated with $\alpha_v\beta_3$ integrin targeting unit and NOTA chelator. The so formed amphiphilic polymer preserved its ability to form unimolecular micelles, capable of pH-controlled drug release via labile hydrazone bond dissociation, and proved suitable for concomitant ^{64}Cu-PET imaging [154]. In an alternative way, the NOTA chelator and anti-CD105 monoclonal antibody (TRC105) have been conjugated with dendritic amphiphilic block copolymers PAMAMePLA-b-PEG, whereas DOX was loaded into the hydrophobic core of the unimolecular micelles formed [182]. Both examples demonstrate a proof-of-principle for cancer theranostic applications of the measured high tumor accumulation of ^{64}Cu-labeled micelles that synergistically integrate the passive and active tumor-targeting with pH-controlled drug release and PET imaging capability. In another approach that progressed to clinical trial (NCT01304797 [183]), ^{64}Cu-labeled chelate based on ATSM was loaded into HER2-targeting PEGylated liposomal doxorubicin (PLD) to form the ^{64}Cu-labeled liposomal therapeutics for PET – [^{64}Cu]Cu-MM-302. This approach allows for non-invasive tracking and quantification of the MM-302 liposome biodistribution and tumor accumulation in patients with HER2-overexpressing breast carcinoma, and can be used for predicting the treatment outcome of liposomal therapy [184].

Other authors have employed the intrinsic affinity of porphyrin conjugates to Cu(II) ions for rapid radiolabeling of different nanosized delivery platforms. Porphyrin-lipid conjugates forming highly stable photonic nanoparticles (porphysomes) have been radiolabeled with ^{64}Cu by a simple and robust direct radiolabeling strategy, thereby obtaining organic nanoparticles suitable for prostate cancer imaging with high chemical stability in the circulation (for at least 30 h) [185]. ^{64}Cu-labeled pentafluorophenylporphyrin complex, [^{64}Cu]Cu-TPPF20, has been grafted on mesoporous silica, MCM-41, functionalized with 3-aminopropyltriethoxysilane, and the evaluation of its biodistribution in fibrosarcoma-bearing rats showed high tumor targeting ability and fast excretion from the body [186]. Furthermore, Zheng and coworkers developed PEGylation-free and porphyrin-based nanoparticles that mimic the nature of lipoproteins, porphylipoprotein (PLP), which are composed of a porphyrin-lipid monolayer, constrained by ApoA-1 mimetic R4F peptide networks that envelopes a hydrophobic drug-loadable cavity [187]. While PLP is highly stable in the blood circulation, even without PEGylation (the high stability is due to the α-helix peptide network that also constrains the PLP size), after tumor accumulation the nanostructures dissociate rapidly to the monomeric fluorescent porphyrins. Thereby, the PLP provides tumor-selective mechanism for low-background NIR fluorescence imaging and photodynamic therapy PDT, since both functionalities are quenched in the intact PLP. Moreover, a facile and efficient ^{64}Cu-labeling of PLP has been achieved through the intrinsic metal chelation ability of porphyrin, which allowed a noninvasive PET imaging of the PLP biodistribution and quantitative assessment of its drug delivery potential. All these features of PLP have been demonstrated on gliosarcoma-bearing mice and indicated a superior

biocompatibility and *in vivo* behavior of PLP than the earlier described porphysomes in terms of rapid intracellular accumulation and PDT activation. The size of the PLP is ~20 nm, which is appropriate to circumvent fast elimination by kidneys (>5 nm) and to allow easy diffusion through the tumor interstitium (<40 nm) – an especially beneficial property to apply in tumors with low permeability. Using a clinically relevant glioblastoma multiforme model, the authors also demonstrated accurate and selective visualization of brain tumor at size <1 mm, proving the potential of PLP for intraoperative fluorescence-guided surgery and tumor-selective PDT. Furthermore, the multimodal cancer imaging by PLP has been evaluated in primary prostate tumors and luciferase-expressing metastatic tumor model by ^{64}Cu-PLP-PET/CT imaging, followed by fluorescence-guided intervention of primary prostate tumor and *ex vivo* fluorescence imaging of suspicious metastatic tumors. All described properties of the biocompatible and nature-inspired PLP make them a unique theranostic nanoplatform for PET and NIR fluorescence imaging, cancer management via imaging-guided surgery and PDT, and potential chemotherapy by utilization of the hydrophobic cavity for drug loading and delivery [187]. It is interesting to note that the topic of light-triggered nanotheranostics (LTN) is of increasing importance in the last years due to their great potential for cancer therapy through integration of selective and light-controlled visualization and treatment of tumors. The large varieties of new and powerful LTNs have recently been summarized, describing the progress in the implementation of various photosensitizers and their performance in complete tumor ablation combined with localized irradiation [188].

A wide variety of nanomaterials suitable for theranostics have been produced on the basis of metallic (or metallic chalcogenide) nanoparticles [179,189]. Among the known ^{64}Cu-labeled magnetic nanoparticles [190], gold nanoparticles [191], upconversion nanoparticles, and inorganic quantum dots [192], the copper sulfide (CuS) nanoparticles are particularly interesting for copper-based nanotheranostics. This is explained with their high intrinsic absorption in the NIR region and high photothermal conversion efficiency that allow for photoacoustic imaging (PAI) and photothermal therapy (PTT). The theranostic potential of such materials has been demonstrated with ultrasmall (8 nm) and uniform CuS-Fn nanocages that had been synthesized inside the cavity of ferritin (Fn) used as biomimetic nanoreactor with a fixed volume [193]. The fast and robust synthesis of these particles using ^{64}Cu radionuclide make them excellent PET imaging agents, providing high tumor accumulation (in the studied U87MG-bearing nude mice) and high photoacoustic contrast and PTT efficacy (at low laser irradiation dose), and low overall toxicity *in vivo* in the dark [193]. Other authors prepared polyethylene glycol-coated [^{64}Cu]CuS NPs that combine the radioimaging (PET) and radiotherapeutic properties of ^{64}Cu with the plasmonic properties of CuS NPs, making them also efficient in the light-controlled PAI and PTT [194]. These PEG-[^{64}Cu]CuS NPs have demonstrated good efficiency in imaging and therapy of anaplastic thyroid carcinoma (ATC) *in vivo* in mice with human Hth83 ATC tumors. The analyses of tumor growth delay and animal survival have indicated that the combined (^{64}Cu) radiotherapy and (CuS) photothermal therapy is highly superior to any of the single therapeutic modalities. In an alternative design, doxorubicin was loaded into hollow mesoporous CuS nanoparticles (HMCuS NPs) and capped with superparamagnetic iron oxide nanoparticles (SPIONPs), thereby combining the chemotherapy with photothermal and photodynamic therapy (PDT) [195]. The SPIONP-caps can be removed by NIR-induced photo-hyperthermia, which provides additional way for external-stimuli controlled drug release. In this case the imaging modality that has been demonstrated is MRI by employing the contrast efficiency of SPIONPs. In another study, the Fe_3O_4 nanoparticles have been self-assembled with PEGylated molybdenum disulfide (MoS_2) nanosheets [190]. They were further modified via chelator-free surface absorption of ^{64}Cu radioisotope for PET imaging. The PEGylated MoS_2–iron oxide (MoS_2-IO) combines three different modalities for both therapy and diagnostics: photothermal ablation of tumors and PAI by the MoS_2 core; magnetic resonance imaging provided by the IO; and precise whole-body ^{64}Cu-PET imaging. Intravenous injection of doubly PEGylated MoS_2-IO-(*d*)PEG followed by laser irradiation resulted in efficient and selective tumor ablation in mice with 4T1 (murine breast cancer) cells [190].

The presented examples are by no means exhaustive, but rather aim to highlight the recent and fast-growing success in the field of copper radiopharmaceuticals. The recently published *"Consensus nomenclature rules for radiopharmaceutical chemistry"* has been applied throughout the text [196]. Moreover, we strongly focused on the design and synthesis of sophisticated multimodal theranostic agents that combine several therapeutic with different imaging modalities and exhibit high efficiency in *in vivo* experiments. The development of numerous molecular and supramolecular nanotheranostic agents, suitable also for advanced bioconjugation and pretargeting approaches, resulted from collaborative interdisciplinary works that have already demonstrated their solid knowledge and productivity. All this gives the hope for successful translation of the discussed nanotheranostic strategies into clinical use.

6. Conclusion

The results accumulated from clinical and preclinical studies on the biomedical application of copper radiopharmaceuticals have demonstrated the high potential of copper radioisotopes for diagnostic imaging as well as for radiotherapy. Despite the high challenges of the task to integrate both functionalities in a single molecular entity, and thereby attain the theranostic application, significant advancement has been achieved.

The solid knowledge on the rich radiochemistry of copper and its coordination properties plays an important role for the observed fast improvement in the development of theranostic copper radiopharmaceuticals. Isotope production methods are in continuous optimization to achieve acceptable cost efficiency, which remains the major obstacle for broader availability of medical radioisotopes of copper; in particular for the therapeutic ^{67}Cu. The efforts to construct ^{62}Zn/^{62}Cu generator come close to commercialization, and production of ^{64}Cu gets even more affordable. Simultaneously, nearly excellent chelators for Cu(II) ions, such as NOTA derivatives, the macrobicyclic CB-TE2A and Sar, have now been established as they provide highly favorable labeling kinetics and essentially high *in vivo* stability of the formed complexes. Many comparative preclinical studies demonstrate the advantages of these three chelators over the broadly used DOTA and TETA. This may suggest that the macrobicyclic chelators or NOTA derivatives should and will be the preferred chelators in the future studies on copper radiopharmaceuticals. Nevertheless, the acyclic ATSM and PTSM remain the most commonly used chelating agents for the very short-lived isotopes ^{60,61,62}Cu because they chelate copper rapidly and their successful application in imaging hypoxia and myocardial perfusion is already demonstrated in several clinical studies. The accumulation of radio-copper in organs that are strongly involved in copper metabolism, such as liver and kidney, remains an issue that can be successfully overcome only by chelators forming complexes of ultrahigh stability; this again suggests the macrobicyclic chelators as a preferable choice. Modulation of the overall charge, hydrophilicity and lipophilicity of the radiopharmaceutical complex are among the additional concerns in assuring its fast clearance from the body.

Significant advancement is already seen in the synthetic procedures that enable the implementation of the pretargeting approaches through bioorthogonal click reactions, and thereby achieve very high specificity in PET imaging as well as in radioimmunotherapy by ^{64}Cu or ^{67}Cu. The preferred biorthogonal click reaction for copper radiopharmaceuticals is the IEDDA reaction as its substrates are stable and relatively easy for synthetic modifications. Preclinical studies on either pretargeted MAbs or supramolecular nanoparticles demonstrate significant advancement in the development of highly specific nanotheranostics based on radio-copper. The high specificity in these cases is achieved either through targeting tumor-specific antigens by suitably modified MAb or through using nanoparticles of appropriate size, which ensures the enhanced permeability and retention (EPR). Furthermore, the methods of nanotechnology for biomimetic construction of biocompatible multimodal copper radiotheranostics appear as a powerful tool to combine either several imaging modalities (e.g. PET/NIR, PET/fluorescence or PET/MRI) or ^{64}Cu-PET and a chemotherapeutic agent (e.g. doxorubicin) included in a supramolecular entity. The latter strategy presents an alternative way to build a theranostic radiopharmaceutical that is able to overcome the dosimetry issues in radioimmunotherapy or the usually high difference in the required radioactivity dose for the imaging and the radiotherapy purposes. Yet, the availability of isotope pairs of copper that are ideal for either imaging or therapy is the main advantage of copper medical isotopes and motivates the ongoing research to optimize the isotopes production methods. Meanwhile, combination of ^{64}Cu and a therapeutic isotope of another metal (e.g. ^{177}Lu) as replaceable radiometals in the same biomolecular vector is one of the evaluated alternatives for building theranostic radiopharmaceuticals. Other approaches employ ^{64}Cu-labeled supramolecular nanoparticles that are able to exert phototherapeutic modes of action, such as photothermal ablation of tumors (by MoS_2 nanosheets of CuS nanoparticles), or photodynamic therapy (by porphysomes and porphylipoproteins).

Undoubtedly, the achievements in the field of copper-based theranostics give not only hope but also interesting suggestions for more advanced strategies to further improve their effectiveness, safety and cost efficiency. The ongoing joint efforts of all specialists in this multidisciplinary field will eventually result in translating into clinical practice the use of copper theranostics for the benefit of patients.

Conflicts of interest

The authors have declared that no conflict of interest exists.

Acknowledgements

Support from H2020-Twinning project (Materials Networking; 692146) is gratefully acknowledged. The authors are thankful for reviewers' very constructive and helpful comments.

Appendix A. Supplementary data

Supplementary data associated with this article can be found in the online version, at https://doi.org/10.1016/j.ejmech.2018.08.051. These data include MOL files and InChiKeys of the most important compounds described in this article.

Abbreviations

ATSM	diacetyl-bis(N4-methylthiosemicarbazone)
PTSM	pyruvaldehyde-bis(N4-methylthiosemicarbazone)
DOTA	1,4,7,10-tetraazadodecane-N,N′,N″,N‴-tetraacetic acid
DOTA-NHS	1,4,7,10-tetraazacyclododecane-N,N′,N″,N‴-tetraacetic acid mono-(N-hydroxy-succinimide ester)
TETA	1,4,8,11- tetraazacyclotetradecane- N,N′,N″,N‴-tetraacetic acid
BAT	6-[p-(bromoacetamido)benzyl]-1,4,7,11-tetraazacyclotetradecane- N,N′,N″,N‴-tetraacetic acid
NOTA	1,4,7-triazacyclononane-1,4,7-triacetic acid
NO2A	1,4,7-triazacyclononane-1,4-diacetic acid
NODAGA	1,4,7-triazacyclononane-1-glutaric acid-4,7 acetic acid
DMPTACN-COOH	2-[4,7-bis(2-pyridylmethyl)-1,4,7-triazacyclononan-1-yl]acetic acid
p-SCN-PhPr-NE3TA	2,2′-(7-(2-((carboxymethyl) (3-(4-iso thiocyanatophenyl)propyl)-amino) ethyl)-1,4,7-triazonane-1,4-diyl) diacetic acid
CPTA	4-(1,4,8,11-tetraazacyclotetradec1-yl)-methyl-benzoic acid tetrachloride
Oxo-DO3A	1-oxa-4,7,10-triazacyclododecane-4,7,10-triacetic acid
PCTA	3,6,9,15-tetraazabicyclo[9.3.1]pentadeca-1(15),11,13-triene-3,6,9-triacetic acid
DO3A	1-(p-nitrobenzyl)-1,4,7,10-tetraazacyclodecane-4,7,10-triacetate
CB-TE2A	cross-bridged 4,11-bis(carboxymethyl)-1,4,8,11-tetraazabicyclo[6.6.2]hexadecane
CB-TE1A1P	cross-bridged 11-carboxymethyl-1,4,8,11-tetraazabicyclo[6.6.2] hexadecane-4-methanephosphonic acid
PCB-TE1A1P	propylene-cross-bridged TETA with hybrid acetate/phosphonate pendant groups
Sar	3,6,10,13,16,19-hexaazabicyclo[6.6.6] icosane
MeCOSar	5-(8-methyl-3,6,10,13,16,19-hexaaza-bicyclo[6.6.6] icosan-1-ylamino)-5-oxopentanoic acid
SarAr	1-N-(4-aminobenzyl)-3,6,10,13,16,19-hexaazabicyclo [6.6.6]-eicosane-1,8-diamine
OC	octreotide
BN or BBN	bombesin
Y3-TATE	Tyr3-octreotate
tetrac	tetraiodothyroacetic acid
LG-Hyd-DOX	L-glutamate-hydrazone-doxorubicin
GGNle-CycMSH$_{hex}$	Gly-Gly-Nle-c[Asp-His-DPhe-Arg-Trp-Lys]-$CONH_2$
6-Ahx	6-aminohexanoic acid
RGD	[Arg-Gly-Asp]
RAFT	regioselectively addressable functionalized template
PACAP	pituitary adenylate cyclase activating peptide
SSTR	Somatostatin receptor
EGFR	endothelial growth factor receptors
HER2	human epidermal growth factor receptor-2
HAEC	human aortic endothelial cells
MAb	monoclonal antibodies
HNC	head-and-neck cancer
NSCLC	non-small-cell lung cancer
NPs	nanoparticles

References

[1] G.S. Patel, T. Kiuchi, K. Lawler, E. Ofo, G.O. Fruhwirth, M. Kelleher, E. Shamil, R. Zhang, P.R. Selvin, G. Santis, J. Spicer, N. Woodman, C.E. Gillett, P.R. Barber, B. Vojnovic, G. Kéri, T. Schaeffter, V. Goh, M.J. O'Doherty, P.A. Ellis, T. Ng, The challenges of integrating molecular imaging into the optimization of cancer therapy, Integr. Biol. 3 (2011) 603–631.

[2] R.N. Krasikova, R.A. Aliev, S.N. Kalmykov, The next generation of positron emission tomography radiopharmaceuticals labeled with non-conventional radionuclides, Mendeleev Commun. 26 (2016) 85–94.

[3] M. Shokeen, T.J. Wadas, The development of copper radiopharmaceuticals for imaging and therapy, Med. Chem. 7 (2011) 413–429.

[4] B.M. Paterson, P.S. Donnelly, Macrocyclic bifunctional chelators and conjugation strategies for Copper-64 radiopharmaceuticals, in: R. van Eldik, C.D. Hubbard (Eds.), Advances in Inorganic Chemistry, Academic Press,

Burlington, 2016, pp. 223–251, https://doi.org/10.1016/bs.adioch.2015.09.005.
[5] P.J. Blower, J.S. Lewis, J. Zweit, Copper radionuclides and radiopharmaceuticals in nuclear medicine, Nucl. Med. Biol. 23 (1996) 957–980.
[6] A. Niccoli Asabella, G.L. Cascini, C. Altini, D. Paparella, A. Notaristefano, G. Rubini, The copper radioisotopes: a systematic review with special interest to ^{64}Cu, BioMed Res. Int. 2014 (2014) 786463.
[7] P. Szymanski, T. Fraczek, M. Markowicz, E. Mikiciuk-Olasik, Development of copper based drugs, radiopharmaceuticals and medical materials, Biometals 25 (2012) 1089–1112.
[8] H.A. Williams, S. Robinson, P. Julyan, J. Zweit, D. Hastings, A comparison of PET imaging characteristics of various copper radioisotopes, Eur. J. Nucl. Med. Mol. Imag. 32 (2005) 1473–1480.
[9] D.W. McCarthy, L.A. Bass, P.D. Cutler, R.E. Shefer, R.E. Klinkowstein, P. Herrero, J.S. Lewis, C.S. Cutler, C.J. Anderson, M.J. Welch, High purity production and potential applications of Copper-60 and Copper-61, Nucl. Med. Biol. 26 (1999) 351–358.
[10] P. Rowshanfarzad, M. Sabet, A.R. Jalilian, M. Kamalidehghan, An overview of copper radionuclides and production of ^{61}Cu by proton irradiation of $^{(nat)}$Zn at a medical cyclotron, Appl. Radiat. Isot. 64 (2006) 1563–1573.
[11] S.S. Das, S. Chattopadhyay, L. Barua, M.K. Das, Production of ^{61}Cu using natural cobalt target and its separation using ascorbic acid and common anion exchange resin, Appl. Radiat. Isot. 70 (2012) 365–368.
[12] T. Fukumura, K. Okada, H. Suzuki, R. Nakao, K. Mukai, F. Szelecsenyi, Z. Kovacs, K. Suzuki, An improved ^{62}Zn/^{62}Cu generator based on a cation exchanger and its fully remote-controlled preparation for clinical use, Nucl. Med. Biol. 33 (2006) 821–827.
[13] D.W. McCarthy, R.E. Shefer, R.E. Klinkowstein, L.A. Bass, W.H. Margeneau, C.S. Cutler, C.J. Anderson, M.J. Welch, Efficient production of high-specific-activity ^{64}Cu using a biomedical cyclotron, Nucl. Med. Biol. 24 (1997) 35–43.
[14] C. Alliot, N. Michel, A.C. Bonraisin, V. Bossé, J. Laizé, C. Bourdeau, B.M. Mokili, F. Haddad, One step purification process for no-Carrier-added ^{64}Cu produced using enriched nickel target, Radiochim. Acta 99 (2011) 627–630.
[15] A. Obata, S. Kasamatsu, D.W. McCarthy, M.J. Welch, H. Saji, Y. Yonekura, Y. Fujibayashi, Production of therapeutic quantities of ^{64}Cu using a 12 MeV cyclotron, Nucl. Med. Biol. 30 (2003) 535–539.
[16] T.J. Wadas, E.H. Wong, G.R. Weisman, C.J. Anderson, Copper chelation chemistry and its role in copper radiopharmaceuticals, Curr. Pharmaceut. Des. 13 (2007) 3–16.
[17] K.R. Zinn, T.R. Chaudhuri, T.-P. Cheng, J.S. Morris, W.A. Meyer Jr., Production of no-Carrier-added ^{64}Cu from zinc metal irradiated under boron shielding, Canc. Metastasis Rev. 73 (1994) 774–778.
[18] S.G. Dolley, T.N. Van Derwalt, G.F. Steyn, F. Szelecsényi, Z. Kovács, The production and isolation of Cu-64 and Cu-67 from zinc target materialand other radionuclides, Czech. J. Phys. 56 (2006) D539–D544.
[19] S.V. Smith, M. Jones, V. Holmes, Production and selection of metal PET radioisotopes for molecular imaging, in: P.N. Sing (Ed.), Radioisotopes - Applications in Bio-medical Science, InTech, 2011. http://www.intechopen.com/books/radioisotopesapplications-in-bio-medical-science/production-and-selection-of-metal-pet-radioisotopes-for-molecular-imaging.
[20] D. Brasse, A. Nonat, Radiometals: towards a new success story in nuclear imaging? Dalton Trans. 44 (2015) 4845–4858.
[21] I. Novak-Hofer, P.A. Schubiger, Copper-67 as a therapeutic nuclide for radioimmunotherapy, Eur. J. Nucl. Med. 29 (2002) 821–830.
[22] T. Katabuchi, S. Watanabe, N.S. Ishioka, Y. Iida, H. Hanaoka, K. Endo, S. Matsuhashi, Production of ^{67}Cu via the ^{68}Zn(p,2p)^{67}Cu reaction and recovery of ^{68}Zn target, J. Radioanal. Nucl. Chem. 277 (2008) 467–470.
[23] N.A. Smith, D.L. Bowers, D.A. Ehst, The production, separation, and use of ^{67}Cu for radioimmunotherapy: a review, Appl. Radiat. Isot. 70 (2012) 2377–2383.
[24] Z. Cai, C.J. Anderson, Chelators for copper radionuclides in positron emission tomography radiopharmaceuticals, J. Labelled Comp. Radiopharm. 57 (2014) 224–230.
[25] T.W. Price, J. Greenman, G.J. Stasiuk, Current advances in ligand design for inorganic positron emission tomography tracers ^{68}Ga, ^{64}Cu, ^{89}Zr and ^{44}Sc, Dalton Trans. 45 (2016) 15702–15724.
[26] E.W. Price, C. Orvig, Matching chelators to radiometals for radiopharmaceuticals, Chem. Soc. Rev. 43 (2014) 260–290.
[27] B.M. Paterson, P.S. Donnelly, Copper complexes of bis(thiosemicarbazones): from chemotherapeutics to diagnostic and therapeutic radiopharmaceuticals, Chem. Soc. Rev. 40 (2011) 3005–3018.
[28] A. Obata, E. Yoshimi, A. Waki, J.S. Lewis, N. Oyama, M.J. Welch, H. Saji, Y. Yonekura, Y. Fujibayashi, Retention mechanism of hypoxia selective nuclear imaging/radiotherapeutic agent Cu-diacetyl-bis(N4-methylthiosemicarbazone) (Cu-ATSM) in tumor cells, Ann. Nucl. Med. 15 (2001) 499–504.
[29] C.F. Ramogida, E. Boros, B.O. Patrick, S.K. Zeisler, J. Kumlin, M.J. Adam, P. Schaffer, C. Orvig, Evaluation of H2CHXdedpa, H2dedpa- and H2CHXdedpa-N,N'-propyl-2-NI ligands for (64)Cu(II) radiopharmaceuticals, Dalton Trans. 45 (2016) 13082–13090.
[30] G.A. Bailey, E.W. Price, B.M. Zeglis, C.L. Ferreira, E. Boros, M.J. Lacasse, B.O. Patrick, J.S. Lewis, M.J. Adam, C. Orvig, H(2)azapa: a versatile acyclic multifunctional chelator for (67)Ga, (64)Cu, (111)In, and (177)Lu, Inorg. Chem. 51 (2012) 12575–12589.
[31] P. Comba, S. Hunoldt, M. Morgen, J. Pietzsch, H. Stephan, H. Wadepohl, Optimization of pentadentate bispidines as bifunctional chelators for ^{64}Cu positron emission tomography (PET), Inorg. Chem. 52 (2013) 8131–8143.
[32] A. Roux, A.M. Nonat, J. Brandel, V. Hubscher-Bruder, L.J. Charbonniere, Kinetically Inert bispidol-based Cu(II) chelate for potential application to (64/67)Cu nuclear medicine and diagnosis, Inorg. Chem. 54 (2015) 4431–4444.
[33] S. Juran, M. Walther, H. Stephan, R. Bergmann, J. Steinbach, W. Kraus, F. Emmerling, P. Comba, Hexadentate bispidine derivatives as versatile bifunctional chelate agents for Copper(II) radioisotopes, Bioconjugate Chem. 20 (2009) 347–359.
[34] G. Park, E. Dadachova, A. Przyborowska, S.-J. Lai, D. Ma, G. Broker, R.D. Rogers, R.P. Planalp, M.W. Brechbiel, Synthesis of novel 1,3,5-cis,cis-triaminocyclohexane ligand based Cu(II) complexes as potential radiopharmaceuticals and correlation of structure and serum stability, Polyhedron 20 (2001) 3155–3163.
[35] D. Ma, F. Lu, T. Overstreet, D.E. Milenic, M.W. Brechbiel, Novel chelating agents for potential clinical applications of copper, Nucl. Med. Biol. 29 (2002) 91–105.
[36] V. Maheshwari, J.L.J. Dearling, S.T. Treves, A.B. Packard, Measurement of the rate of copper(II) exchange for ^{64}Cu complexes of bifunctional chelators, Inorg. Chim. Acta. 393 (2012) 318–323.
[37] K. Zarschler, M. Kubeil, H. Stephan, Establishment of two complementary in vitro assays for radiocopper complexes achieving reliable and comparable evaluation of in vivo stability, RSC Adv. 4 (2014) 10157–10164.
[38] M. Kubeil, K. Zarschler, J. Pietzsch, W. Kraus, P. Comba, H. Stephan, Copper(II) cyclam complexes with n-propionic acid pendant arms, Eur. J. Inorg. Chem. 2015 (2015) 4013–4023.
[39] A. Rodriguez-Rodriguez, Z. Halime, L.M. Lima, M. Beyler, D. Deniaud, N. Le Poul, R. Delgado, C. Platas-Iglesias, V. Patinec, R. Tripier, Cyclams with ambidentate methylthiazolyl pendants for stable, inert, and selective Cu(II) coordination, Inorg. Chem. 55 (2016) 619–632.
[40] A. Rodriguez-Rodriguez, Z. Garda, E. Ruscsak, D. Esteban-Gomez, A. de Blas, T. Rodriguez-Blas, L.M. Lima, M. Beyler, R. Tripier, G. Tircso, C. Platas-Iglesias, Stable Mn(2+), Cu(2+) and Ln(3+) complexes with cyclen-based ligands functionalized with picolinate pendant arms, Dalton Trans. 44 (2015) 5017–5031.
[41] L.M. Lima, D. Esteban-Gomez, R. Delgado, C. Platas-Iglesias, R. Tripier, Monopicolinate cyclen and cyclam derivatives for stable copper(II) complexation, Inorg. Chem. 51 (2012) 6916–6927.
[42] X. Sun, M. Wuest, Z. Kovacs, A.D. Sherry, R. Motekaitis, Z. Wang, A.E. Martell, M.J. Welch, C.J. Anderson, In vivo behavior of copper-64-labeled methanephosphonate tetraaza macrocyclic ligands, J. Biol. Inorg. Chem. 8 (2003) 217–225.
[43] C.L. Ferreira, D.T. Yapp, E. Lamsa, M. Gleave, C. Bensimon, P. Jurek, G.E. Kiefer, Evaluation of novel bifunctional chelates for the development of Cu-64-based radiopharmaceuticals, Nucl. Med. Biol. 35 (2008) 875–882.
[44] S. Ait-Mohand, P. Fournier, V. Dumulon-Perreault, G.E. Kiefer, P. Jurek, C.L. Ferreira, F. Benard, B. Guerin, Evaluation of ^{64}Cu-labeled bifunctional Chelate-Bombesin conjugates, Bioconjugate Chem. 22 (2011) 1729–1735.
[45] W.M. Rockey, L. Huang, K.C. Kloepping, N.J. Baumhover, P.H. Giangrande, M.K. Schultz, Synthesis and radiolabeling of chelator-RNA aptamer bioconjugates with copper-64 for targeted molecular imaging, Bioorg. Med. Chem. 19 (2011) 4080–4090.
[46] C.L. Ferreira, D.T.T. Yapp, S. Crisp, B.W. Sutherland, S.W. Ng Sylvia, M. Gleave, C. Bensimon, P. Jurek, G.E. Kiefer, Comparison of bifunctional chelates for (64)Cu antibody imaging, Eur. J. Nucl. Med. Mol. Imag. 37 (2010) 2117–2126.
[47] M.S. Cooper, M.T. Ma, K. Sunassee, K.P. Shaw, J.D. Williams, R.L. Paul, P.S. Donnelly, P.J. Blower, Comparison of 64cu-complexing bifunctional chelators for radioimmunoconjugation: labeling efficiency, specific activity, and in vitro/in vivo stability, Bioconjugate Chem. 23 (2012) 1029–1039.
[48] I.H. Song, T.S. Lee, Y.S. Park, J.S. Lee, B.C. Lee, B.S. Moon, G.I. An, H.W. Lee, K.I. Kim, Y.J. Lee, J.H. Kang, S.M. Lim, Immuno-PET imaging and radioimmunotherapy of ^{64}Cu-/^{177}Lu-labeled anti-EGFR antibody in esophageal squamous cell carcinoma model, J. Nucl. Med. 57 (2016) 1105–1111.
[49] G.R. Weisman, E.H. Wong, D.C. Hill, M.E. Rogers, D.P. Reed, J.C. Calabrese, Synthesis and transition-metal complexes of new cross-bridged tetraamine ligands, J. Chem. Soc., Chem. Commun. (1996) 947–948.
[50] E.H. Wong, G.R. Weisman, D.C. Hill, D.P. Reed, M.E. Rogers, J.P. Condon, M.A. Fagan, J.C. Calabrese, K.C. Lam, I.A. Guzei, A.L. Rheingold, Synthesis and characterization of cross-bridged cyclams and pendant-armed derivatives and structural studies of their copper(II) complexes, J. Am. Chem. Soc. 122 (2000) 10561–10572.
[51] C.A. Boswell, X. Sun, W. Niu, G.R. Weisman, E.H. Wong, A.L. Rheingold, C.J. Anderson, Comparative in vivo stability of Copper-64-labeled cross-bridged and conventional tetraazamacrocyclic complexes, J. Med. Chem. 47 (2004) 1465–1474.
[52] E.A. Lewis, R.W. Boyle, S.J. Archibald, Ultrastable complexes for in vivo use: a bifunctional chelator incorporating a cross-bridged macrocycle, Chem. Commun. (2004) 2212–2213.
[53] J.D. Silversides, C.C. Allan, S.J. Archibald, Copper(II) cyclam-based complexes for radiopharmaceutical applications: synthesis and structural analysis, Dalton Trans. (2007) 971–978.
[54] J.D. Silversides, R. Smith, S.J. Archibald, Challenges in chelating positron emitting copper isotopes: tailored synthesis of unsymmetric chelators to form ultra stable complexes, Dalton Trans. 40 (2011) 6289–6297.
[55] C.A. Boswell, C.A.S. Regino, K.E. Baidoo, K.J. Wong, A. Bumb, H. Xu,

D.E. Milenic, J.A. Kelley, C.C. Lai, M.W. Brechbiel, Synthesis of a cross-bridged cyclam derivative for peptide conjugation and ^{64}Cu radiolabeling, Bioconjugate Chem. 19 (2008) 1476–1484.
[56] X. Sun, M. Wuest, G.R. Weisman, E.H. Wong, D.P. Reed, C.A. Boswell, R. Motekaitis, A.E. Martell, M.J. Welch, C.J. Anderson, Radiolabeling and in vivo behavior of copper-64-labeled cross-bridged cyclam ligands, J. Med. Chem. 45 (2002) 469–477.
[57] J.E. Sprague, Y. Peng, X. Sun, G.R. Weisman, E.H. Wong, S. Achilefu, C.J. Anderson, Preparation and biological evaluation of copper-64-labeled Tyr 3-octreotate using a cross-bridged macrocyclic chelator, Clin. Canc. Res. 10 (2004) 8674–8682.
[58] T.J. Wadas, M. Eiblmaier, A. Zheleznyak, C.D. Sherman, R. Ferdani, K. Liang, S. Achilefu, C.J. Anderson, Preparation and biological evaluation of ^{64}Cu-CB-TE2A-sst 2-ANT, a somatostatin antagonist for PET imaging of somatostatin receptor-positive tumors, J. Nucl. Med. 49 (2008) 1819–1827.
[59] C.V. Esteves, J. Madureira, L.M. Lima, P. Mateus, I. Bento, R. Delgado, Copper(II) and gallium(III) complexes of trans-bis(2-hydroxybenzyl) cyclen derivatives: absence of a cross-bridge proves surprisingly more favorable, Inorg. Chem. 53 (2014) 4371–4386.
[60] C.V. Esteves, P. Lamosa, R. Delgado, J. Costa, P. Desogere, Y. Rousselin, C. Goze, F. Denat, Remarkable inertness of copper(II) chelates of cyclen-based macrobicycles with two trans-N-acetate arms, Inorg. Chem. 52 (2013) 5138–5153.
[61] E. Boros, E. Rybak-Akimova, J.P. Holland, T. Rietz, N. Rotile, F. Blasi, H. Day, R. Latifi, P. Caravan, Pycup-a bifunctional, cage-like ligand for (64)Cu radiolabeling, Mol. Pharm. 11 (2014) 617–629.
[62] Z. Liu, Z.-B. Li, Q. Cao, S. Liu, F. Wang, X. Chen, Small-animal PET of tumors with ^{64}Cu-labeled RGD-bombesin heterodimer, J. Nucl. Med. 50 (2009) 1168–1177.
[63] D. Liu, D. Overbey, L.D. Watkinson, C.J. Smith, S. Daibes-Figueroa, T.J. Hoffman, L.R. Forte, W.A. Volkert, M.F. Giblin, Comparative evaluation of three ^{64}Cu-labeled E. coli heat-stable enterotoxin analogues for PET imaging of colorectal cancer, Bioconjugate Chem. 21 (2010) 1171–1176.
[64] R.A. De Silva, S. Jain, K.A. Lears, H.S. Chong, C.S. Kang, X. Sun, B.E. Rogers, Copper-64 radiolabeling and biological evaluation of bifunctional chelators for radiopharmaceutical development, Nucl. Med. Biol. 39 (2012) 1099–1104.
[65] S.R. Kumar, F.A. Gallazzi, R. Ferdani, C.J. Anderson, T.P. Quinn, S.L. Deutscher, In vitro and in vivo evaluation of 64Cu-radiolabeled kccysl peptides for targeting epidermal growth factor receptor-2 in breast carcinomas, Cancer Biother, Radiopharm 25 (2010) 693–703.
[66] I. Sin, C.S. Kang, N. Bandara, X. Sun, Y. Zhong, B.E. Rogers, H.-S. Chong, Novel hexadentate and pentadentate chelators for ^{64}Cu-based targeted PET imaging, Bioorg. Med. Chem. 22 (2014) 2553–2562.
[67] M. Moreau, S. Poty, J.M. Vrigneaud, P. Walker, M. Guillemin, O. Raguin, A. Oudot, C. Bernhard, C. Goze, F. Boschetti, B. Collin, F. Brunotte, F. Denat, MANOTA: a promising bifunctional chelating agent for copper-64 immunoPET, Dalton Trans. 46 (2017) 14659–14668.
[68] R.J. Geue, A.M. Sargeson, T.W. Hambley, M.R. Snow, J.M. Harrowfield, Metal ion encapsulation: cobalt cages derived from polyamines, formaldehyde, and nitromethane, J. Am. Chem. Soc. 106 (1984) 5478–5488.
[69] R.J. Geue, B. Korybut-Daszkiewicz, A.M. Sargeson, A new reagent for synthesis of cages for metal ions, J. Chem. Soc., Chem. Commun. (1993) 1454–1456.
[70] N.M. Di Bartolo, A.M. Sargeson, T.M. Donlevy, S.V. Smith, Synthesis of a new cage ligand, SarAr, and its complexation with selected transition metal ions for potential use in radioimaging, J. Chem. Soc., Dalton Trans. (2001) 2303–2309.
[71] N. Di Bartolo, A.M. Sargeson, S.V. Smith, New 64Cu PET imaging agents for personalised medicine and drug development using the hexa-aza cage, SarAr, Org. Biomol. Chem. 4 (2006) 3350–3357.
[72] S.D. Voss, S.V. Smith, N. Dibartolo, L.J. McIntosh, E.M. Cyr, A.A. Bonab, J.L.J. Dearling, E.A. Carter, A.J. Fischman, S.T. Treves, S.D. Gillies, A.M. Sargeson, J.S. Huston, A.B. Packard, Positron emission tomography (PET) imaging of neuroblastoma and melanoma with 64Cu-SarAr immunoconjugates, Proc. Natl. Acad. Sci. U.S.A. 104 (2007) 17489–17493.
[73] E. Mume, A. Asad, N.M. Di Bartolo, L. Kong, C. Smith, A.M. Sargeson, R. Price, S.V. Smith, Synthesis of hexa aza cages, SarAr-NCS and AmBaSar and a study of their metal complexation, conjugation to nanomaterials and proteins for application in radioimaging and therapy, Dalton Trans. 42 (2013) 14402–14410.
[74] L. Wei, Y. Ye, T.J. Wadas, J.S. Lewis, M.J. Welch, S. Achilefu, C.J. Anderson, 64) Cu-labeled CB-TE2A and diamsar-conjugated RGD peptide analogs for targeting angiogenesis: comparison of their biological activity, Nucl. Med. Biol. 36 (2009) 277–285.
[75] Z. Wu, S. Liu, I. Nair, K. Omori, S. Scott, I. Todorov, J.E. Shively, P.S. Conti, Z. Li, F. Kandeel, ^{64}Cu labeled sarcophagine exendin-4 for microPET imaging of glucagon like peptide-1 receptor expression, Theranostics 4 (2014) 770–777.
[76] S. Liu, Z. Li, P.S. Conti, Development of multi-functional chelators based on sarcophagine cages, Molecules 19 (2014) 4246–4255.
[77] J.L.J. Dearling, B.M. Paterson, V. Akurathi, S. Betanzos-Lara, S.T. Treves, S.D. Voss, J.M. White, J.S. Huston, S.V. Smith, P.S. Donnelly, A.B. Packard, The ionic charge of copper-64 complexes conjugated to an engineered antibody affects biodistribution, Bioconjugate Chem. 26 (2015) 707–717.
[78] S. Liu, Z. Li, L.P. Yap, C.W. Huang, R. Park, P.S. Conti, Efficient preparation and biological evaluation of a novel multivalency bifunctional chelator for ^{64}Cu radiopharmaceuticals, Chem. Eur J. 17 (2011) 10222–10225.
[79] J.P. Meyer, P. Adumeau, J.S. Lewis, B.M. Zeglis, Click chemistry and radiochemistry: the first 10 years, Bioconjugate Chem. 27 (2016) 2791–2807.
[80] Z. Cai, B.T. Li, E.H. Wong, G.R. Weisman, C.J. Anderson, Cu(I)-assisted click chemistry strategy for conjugation of non-protected cross-bridged macrocyclic chelators to tumour-targeting peptides, Dalton Trans. 44 (2015) 3945–3948.
[81] E.M. Sletten, C.R. Bertozzi, Bioorthogonal chemistry: fishing for selectivity in a sea of functionality, Angew. Chem. Int. Ed. 48 (2009) 6974–6998.
[82] S. Liu, D. Li, R. Park, R. Liu, Z. Xia, J. Guo, V. Krasnoperov, P.S. Gill, Z. Li, H. Shan, P.S. Conti, PET imaging of colorectal and breast cancer by targeting EphB4 receptor with ^{64}Cu-labeled hAb47 and hAb131 antibodies, J. Nucl. Med. 54 (2013) 1094–1100.
[83] K. Chen, X. Wang, W.Y. Lin, C.K. Shen, L.P. Yap, L.D. Hughes, P.S. Conti, Strain-Promoted Catalyst-Free click chemistry for rapid construction of (64)Cu-Labeled PET imaging probes, ACS Med. Chem. Lett. 3 (2012) 1019–1023.
[84] B.E. Cook, P. Adumeau, R. Membreno, K.E. Carnazza, C. Brand, T. Reiner, B.J. Agnew, J.S. Lewis, B.M. Zeglis, Pretargeted PET imaging using a site-specifically labeled immunoconjugate, Bioconjugate Chem. 27 (2016) 1789–1795.
[85] B.M. Zeglis, C. Brand, D. Abdel-Atti, K.E. Carnazza, B.E. Cook, S. Carlin, T. Reiner, J.S. Lewis, Optimization of a pretargeted strategy for the PET imaging of colorectal carcinoma via the modulation of radioligand pharmacokinetics, Mol. Pharm. 12 (2015) 3575–3587.
[86] J.L. Houghton, B.M. Zeglis, D. Abdel-Atti, R. Sawada, W.W. Scholz, J.S. Lewis, Pretargeted immuno-PET of pancreatic cancer: overcoming circulating antigen and internalized antibody to reduce radiation doses, J. Nucl. Med. 57 (2016) 453–459.
[87] S. Hou, J.S. Choi, M.A. Garcia, Y. Xing, K.J. Chen, Y.M. Chen, Z.K. Jiang, T. Ro, L. Wu, D.B. Stout, J.S. Tomlinson, H. Wang, K. Chen, H.R. Tseng, W.Y. Lin, Pretargeted positron emission tomography imaging that employs supramolecular nanoparticles with in vivo bioorthogonal chemistry, ACS Nano 10 (2016) 1417–1424.
[88] P. Adumeau, K.E. Carnazza, C. Brand, S.D. Carlin, T. Reiner, B.J. Agnew, J.S. Lewis, B.M. Zeglis, A pretargeted approach for the multimodal PET/NIRF imaging of colorectal cancer, Theranostics 6 (2016) 2267–2277.
[89] B.M. Zeglis, P. Mohindra, G.I. Weissmann, V. Divilov, S.A. Hilderbrand, R. Weissleder, J.S. Lewis, Modular strategy for the construction of radiometalated antibodies for positron emission tomography based on inverse electron demand diels-alder click chemistry, Bioconjugate Chem. 22 (2011) 2048–2059.
[90] S.V. Govindan, D.M. Goldenberg, H.J. Hansen, G.L. Griffiths, Advances in the use of monoclonal antibodies in cancer radiotherapy, Pharmaceut. Sci. Technol. Today 3 (2000) 90–98.
[91] M. Patra, K. Zarschler, H.J. Pietzsch, H. Stephan, G. Gasser, New insights into the pretargeting approach to image and treat tumours, Chem. Soc. Rev. 45 (2016) 6415–6431.
[92] C. Bailly, C. Bodet-Milin, C. Rousseau, A. Faivre-Chauvet, F. Kraeber-Bodéré, J. Barbet, Pretargeting for imaging and therapy in oncological nuclear medicine, EJNMMI Radiopharm. Chem. 2 (2017) 6, https://doi.org/10.1186/s41181-017-0026-8.
[93] S.J. Knox, M.L. Goris, M. Tempero, P.L. Weiden, L. Gentner, H. Breitz, G.P. Adams, D. Axworthy, S. Gaffigan, K. Bryan, D.R. Fisher, D. Colcher, I.D. Horak, L.M. Weiner, Phase II trial of Yttrium-90-DOTA-Biotin pretargeted by NR-LU-10 antibody/streptavidin in patients with metastatic colon cancer, Clin. Canc. Res. 6 (2000) 406–414.
[94] R. Schoffelen, O.C. Boerman, D.M. Goldenberg, R.M. Sharkey, C.M. van Herpen, G.M. Franssen, W.J. McBride, C.H. Chang, E.A. Rossi, W.T. van der Graaf, W.J. Oyen, Development of an imaging-guided CEA-pretargeted radionuclide treatment of advanced colorectal cancer: first clinical results, Br. J. Canc. 109 (2013) 934–942.
[95] F. Kraeber-Bodéré, C. Rousseau, C. Bodet-Milin, E. Frampas, A. Faivre-Chauvet, A. Rauscher, R.M. Sharkey, D.M. Goldenberg, J.F. Chatal, J. Barbet, A pretargeting system for tumor PET imaging and radioimmunotherapy, Front. Pharmacol. 6 (2015) 54, https://doi.org/10.3389/fphar.2015.00054.
[96] P. Adumeau, S.K. Sharma, C. Brent, B.M. Zeglis, Site-specifically labeled immunoconjugates for molecular imaging-Part 1: cysteine residues and Glycans, Mol. Imag. Biol. 18 (2016) 1–17.
[97] P. Adumeau, S.K. Sharma, C. Brent, B.M. Zeglis, Site-specifically labeled immunoconjugates for molecular imaging-Part 2: peptide tags and unnatural amino acids, Mol. Imag. Biol. 18 (2016) 153–165.
[98] https://clinicaltrials.gov/ct2/results?term=64Cu, clinical trials on 64Cu.
[99] https://clinicaltrials.gov/ct2/results?term=62Cu, clinical trilas on 62Cu.
[100] F. Dehdashti, M.A. Mintun, J.S. Lewis, J. Bradley, R. Govindan, R. Laforest, M.J. Welch, B.A. Siegel, In vivo assessment of tumor hypoxia in lung cancer with ^{60}Cu-ATSM, Eur. J. Nucl. Med. Mol. Imag. 30 (2003) 844–850.
[101] P.W. Grigsby, R.S. Malyapa, R. Higashikubo, J.K. Schwarz, M.J. Welch, P.C. Huettner, F. Dehdashti, Comparison of molecular markers of hypoxia and imaging with ^{60}Cu-ATSM in cancer of the uterine cervix, Mol. Imag. Biol. 9 (2007) 278–283.
[102] F. Dehdashti, P.W. Grigsby, J.S. Lewis, R. Laforest, B.A. Siegel, M.J. Welch, Assessing tumor hypoxia in cervical cancer by PET with ^{60}Cu- labeled diacetyl-bis(N4-methylthiosemicarbazone), J. Nucl. Med. 49 (2008) 201–205.

[103] A. Kositwattanarerk, M. Oh, T. Kudo, Y. Kiyono, T. Mori, Y. Kimura, R. Maruyama, Y. Fujibayashi, S. Fujieda, H. Okazawa, Different distribution of ^{62}Cu ATSM and ^{18}F-FDG in head and neck cancers, Clin. Nucl. Med. 37 (2012) 252–257.

[104] Y. Sato, T. Tsujikawa, M. Oh, T. Mori, Y. Kiyono, S. Fujieda, H. Kimura, H. Okazawa, Assessing tumor hypoxia in head and neck cancer by PET with 62Cu-Diacetyl-Bis(N4-methylthiosemicarbazone), Clin. Nucl. Med. 39 (2014) 1027–1032.

[105] K. Tateishi, U. Tateishi, M. Sato, S. Yamanaka, H. Kanno, H. Murata, T. Inoue, N. Kawahara, Application of ^{62}Cu-diacetyl-bis (N4-methylthiosemicarbazone) PET imaging to predict highly malignant tumor grades and hypoxia-inducible factor-1alpha expression in patients with glioma, AJNR Am. J. Neuroradiol. 34 (2013) 92–99.

[106] K. Tateishi, U. Tateishi, S. Nakanowatari, M. Ohtake, R. Minamimoto, J. Suenaga, H. Murata, K. Kubota, T. Inoue, N. Kawahara, (62)Cu-diacetyl-bis (N(4)-methylthiosemicarbazone) PET in human gliomas: comparative study with (18)F-fluorodeoxyglucose and L-methyl-(11)C-methionine PET, AJNR Am. J. Neuroradiol. 35 (2014) 278–284.

[107] N.G. Haynes, J.L. Lacy, N. Nayak, C.S. Martin, D. Dai, C.J. Mathias, M.A. Green, Performance of a ^{62}Zn/^{62}Cu generator in clinical trials of PET perfusion agent ^{62}Cu-PTSM, J. Nucl. Med. 41 (2000) 309–314.

[108] T.R. Wallhaus, J. Lacy, R. Stewart, J. Bianco, M.A. Green, N. Nayak, C.K. Stone, Copper-62-pyruvaldehyde bis(N4-methyl-thiosemicarbazone) PET imaging in the detection of coronary artery disease in humans, J. Nucl. Cardiol. 8 (2001) 67–74.

[109] T.Z. Wong, J.L. Lacy, N.A. Petry, T.C. Hawk, T.A. Sporn, M.W. Dewhirst, G. Vlahovic, PET of hypoxia and perfusion with ^{62}Cu-ATSM and ^{62}Cu-PTSM using a ^{62}Zn/^{62}Cu generator, Am. J. Roentgenol. 190 (2008) 427–432.

[110] T. Zhang, S.K. Das, D.R. Fels, K.S. Hansen, T.Z. Wong, M.W. Dewhirst, G. Vlahovic, PET with ^{62}Cu-ATSM and ^{62}Cu-PTSM is a useful imaging tool for hypoxia and perfusion in pulmonary lesions, Am. J. Roentgenol. 201 (2013) W698–W706.

[111] R. Chakravarty, S. Chakraborty, A. Dash, $^{64}Cu^{2+}$ Ions as PET Probe: an emerging paradigm in molecular imaging of cancer, Mol. Pharm. 13 (2016) 3601–3612.

[112] E. Capasso, S. Durzu, S. Piras, S. Zandieh, P. Knoll, A. Haug, M. Hacker, C. Meleddu, S. Mirzaei, Role of $^{64}CuCl_2$ PET/CT in staging of prostate cancer, Ann. Nucl. Med. 29 (2015) 482–488.

[113] P. Panichelli, C. Villano, A. Cistaro, A. Bruno, F. Barbato, A. Piccardo, A. Duatti, Imaging of brain tumors with Copper-64 chloride: early experience and results, Cancer Biother. Radiopharm. 31 (2016) 159–167.

[114] C. Qin, H. Liu, K. Chen, X. Hu, X. Ma, X. Lan, Y. Zhang, Z. Cheng, Theranostics of malignant melanoma with $^{64}CuCl_2$, J. Nucl. Med. 55 (2014) 812–817.

[115] J.S. Lewis, R. Laforest, F. Dehdashti, P.W. Grigsby, M.J. Welch, B.A. Siegel, An imaging comparison of ^{64}Cu-ATSM and ^{60}Cu-ATSM in cancer of the uterine cervix, J. Nucl. Med. 49 (2008) 1177–1182.

[116] E. Lopci, I. Grassi, D. Rubello, P.M. Colletti, S. Cambioli, A. Gamboni, F. Salvi, G. Cicoria, F. Lodi, C. Dazzi, S. Mattioli, S. Fanti, Prognostic evaluation of disease outcome in solid tumors investigated with ^{64}Cu-ATSM PET/CT, Clin. Nucl. Med. 41 (2016) e87–e92.

[117] M.L. Thakur, K. Zhang, A. Berger, B. Cavanaugh, S. Kim, C. Channappa, A.J. Frangos, E. Wickstrom, C.M. Intenzo, VPAC1 receptors for imaging breast cancer: a feasibility study, J. Nucl. Med. 54 (2013) 1019–1025.

[118] S. Tripathi, E.J. Trabulsi, L. Gomella, S. Kim, P. McCue, C. Intenzo, R. Birbe, A. Gandhe, P. Kumar, M. Thakur, VPAC1 targeted (64)Cu-TP3805 positron emission tomography imaging of prostate cancer: preliminary evaluation in man, Urology 88 (2016) 111–118.

[119] J.L. Hickey, S. Lim, D.J. Hayne, B.M. Paterson, J.M. White, V.L. Villemagne, P. Roselt, D. Binns, C. Cullinane, C.M. Jeffery, R.I. Price, K.J. Barnham, P.S. Donnelly, Diagnostic imaging agents for alzheimer's disease: copper radiopharmaceuticals that target Aβ-plaques, J. Am. Chem. Soc. 135 (2013) 16120–16132.

[120] C.J. Anderson, F. Dehdashti, P.D. Cutler, S.W. Schwarz, R. Laforest, L.A. Bass, J.S. Lewis, D.W. McCarthy, ^{64}Cu-TETA-octreotide as a PET imaging agent for patients with neuroendocrine tumors, J. Nucl. Med. 42 (2001) 213–221.

[121] C.J. Anderson, L.A. Jones, L.A. Bass, E.L.C. Sherman, D.W. McCarthy, P.D. Cutler, M.V. Lanahan, M.E. Cristel, J.S. Lewis, S.W. Schwarz, Radiotherapy, toxicity and dosimetry of copper-64-TETA-octreotide in tumor-bearing rats, J. Nucl. Med. 39 (1998) 1944–1951.

[122] J.S. Lewis, M.R. Lewis, P.D. Cutler, A. Srinivasan, M.A. Schmidt, S.W. Schwarz, M.M. Morris, J.P. Miller, C.J. Anderson, Radiotherapy and dosimetry of ^{64}Cu-TETA-Tyr3-octreotate in a somatostatin receptor-positive, tumor-bearing rat model, Clin. Canc. Res. 5 (1999) 3608–3616.

[123] H. Zhang, K. Abiraj, D.L.J. Thorek, B. Waser, P.M. Smith-Jones, M. Honer, J.C. Reubi, H.R. Maecke, Evolution of bombesin conjugates for targeted PET imaging of tumors, PLoS One 7 (2012), e44046, https://doi.org/10.44010.41371/journal.pone.0044046.

[124] H. Wang, W. Cai, K. Chen, Z.-B. Li, A. Kashefi, L. He, X. Chen, A new PET tracer specific for vascular endothelial growth factor receptor 2, Eur. J. Nucl. Med. Mol. Imag. 34 (2007) 2001–2010.

[125] X. Chen, R. Park, M. Tohme, A.H. Shahinian, J.R. Bading, P.S. Conti, MicroPET and autoradiographic imaging of breast cancer $\alpha_v\beta_3$-integrin expression using ^{18}F- and ^{64}Cu-labeled RGD peptide, Bioconjugate Chem. 15 (2004) 41–49.

[126] F. Cao, Z. Li, A. Lee, Z. Liu, K. Chen, H. Wang, C. Weibo, X. Chen, J.C. Wu, Noninvasive de novo imaging of human embryonic stem cell-derived teratoma formation, Canc. Res. 69 (2009) 2709–2713.

[127] K. Chen, W. Ma, G. Li, J. Wang, W. Yang, L.-P. Yap, L.D. Hughes, R. Park, P.S. Conti, Synthesis and evaluation of ^{64}Cu-labeled monomeric and dimeric NGR peptides for MicroPET imaging of CD13 receptor expression, Mol. Pharm. 10 (2013) 417–427.

[128] K. Chen, X. Sun, G. Niu, Y. Ma, L.-P. Yap, X. Hui, K. Wu, D. Fan, P.S. Conti, X. Chen, Evaluation of ^{64}Cu labeled GX1: a phage display peptide probe for PET imaging of tumor vasculature, Mol. Imag. Biol. 14 (2012) 96–105.

[129] H. Deng, H. Wang, M. Wang, Z. Li, Z. Wu, Synthesis and evaluation of ^{64}Cu-DOTA-NT-Cy5.5 as a dual-modality pet/fluorescence probe to image neurotensin receptor-positive tumor, Mol. Pharm. 12 (2015) 3054–3061.

[130] F. Li, S. Jiang, Y. Zu, D.Y. Lee, Z. Li, A tyrosine kinase inhibitor-based high-affinity PET radiopharmaceutical targets vascular endothelial growth factor receptor, J. Nucl. Med. 55 (2014) 1525–1531.

[131] C.M. Kang, H.J. Koo, S. Lee, K.C. Lee, Y.K. Oh, Y.S. Choe, ^{64}Cu-Labeled tetraiodothyro-acetic acid-conjugated liposomes for PET imaging of tumor angiogenesis, Nucl. Med. Biol. 40 (2013) 1018–1024.

[132] A.L. Petersen, T. Binderup, R.I. Jolck, P. Rasmussen, J.R. Henriksen, A.K. Pfeifer, A. Kjaer, T.L. Andresen, Positron emission tomography evaluation of somatostatin receptor targeted ^{64}Cu-TATE-liposomes in a human neuroendocrine carcinoma mouse model, J. Contr. Release 160 (2012) 254–263.

[133] S. Liu, D. Li, J. Guo, N. Canale, X. Li, R. Liu, V. Krasnoperov, P.S. Gill, P.S. Conti, H. Shan, Z. Li, Design, synthesis, and validation of Axl-targeted monoclonal antibody probe for microPET imaging in human lung cancer xenograft, Mol. Pharm. 11 (2014) 3974–3979.

[134] K. Higashikawa, K. Yagi, K. Watanabe, S. Kamino, M. Ueda, M. Hiromura, S. Enomoto, 64Cu-DOTA-anti-CTLA-4 mAb enabled PET visualization of CTLA-4 on the T-cell infiltrating tumor tissues, PLoS One 9 (2014), e109866, https://doi.org/10.1371/journal.pone.0109866.

[135] H. Wang, D. Li, S. Liu, R. Liu, H. Yuan, V. Krasnoperov, H. Shan, P.S. Conti, P.S. Gill, Z. Li, Small-animal pet imaging of pancreatic cancer xenografts using a ^{64}Cu-labeled monoclonal antibody, MAb159, J. Nucl. Med. 56 (2015) 908–913.

[136] C. Schjoeth-Eskesen, C.H. Nielsen, S. Heissel, P. Hojrup, P.R. Hansen, N. Gillings, A. Kjaer, 64)Cu-labelled trastuzumab: optimisation of labelling by DOTA and NODAGA conjugation and initial evaluation in mice, J. Labelled Comp. Radiopharm. 58 (2015) 227–233.

[137] A. Natarajan, N. Arksey, A. Iagaru, F.T. Chin, S.S. Gambhir, Validation of 64Cu-DOTA-rituximab injection preparation under good manufacturing practices: a PET tracer for imaging of B-cell non-Hodgkin lymphoma, Mol. Imag. 14 (2015), https://doi.org/10.2310/7290.2014.00055.

[138] A. Natarajan, B.J. Hackel, S.S. Gambhir, A novel engineered anti-CD20 tracer enables early time PET imaging in a humanized transgenic mouse model of b-cell non-hodgkins lymphoma, Clin. Canc. Res. 19 (2013) 6820–6829.

[139] S. Nittka, M.A. Krueger, J.E. Shively, H. Boll, M.A. Brockmann, F. Doyon, B.J. Pichler, M. Neumaier, Radioimmunoimaging of liver metastases with PET using a ^{64}Cu-labeled CEA antibody in transgenic mice, PLoS One 9 (2014), e106921, https://doi.org/10.1371/journal.pone.0106921.

[140] Y. Guo, J.J. Parry, R. Laforest, B.E. Rogers, C.J. Anderson, The role of p53 in combination radioimmunotherapy with ^{64}Cu- DOTA-cetuximab and cisplatin in a mouse model of colorectal cancer, J. Nucl. Med. 54 (2013) 1621–1629.

[141] L. Xiao, Y. Zhang, Z. Yang, Y. Xu, B. Kundu, M.D. Chordia, D. Pan, Synthesis of PECAM-1-specific ^{64}Cu PET imaging agent: evaluation of myocardial infarction caused by ischemia-reperfusion injury in mouse, Bioorg. Med. Chem. Lett 22 (2012) 4144–4147.

[142] I. Nakamura, K. Hasegawa, Y. Wada, T. Hirase, K. Node, Y. Watanabe, Detection of early stage atherosclerotic plaques using PET and CT fusion imaging targeting P-selectin in low density lipoprotein receptor-deficient mice, Biochem. Biophys. Res. Commun. 433 (2013) 47–51.

[143] D. McLean, M.J. Cooke, R. Albay III, C. Glabe, M.S. Shoichet, Positron emission tomography imaging of fibrillar parenchymal and vascular amyloid-β in TgCRND8 mice, ACS Chem. Neurosci. 4 (2013) 613–623.

[144] R. Rossin, S. Muro, M.J. Welch, V.R. Muzykantov, D.P. Schustery, In vivo imaging of ^{64} Cu-labeled polymer nanoparticles targeted to the lung endothelium, J. Nucl. Med. 49 (2008) 103–111.

[145] M.H. Kim, S.K. Woo, K.I. Kim, T.S. Lee, C.W. Kim, J.H. Kang, B.I. Kim, S.M. Lim, K.C. Lee, Y.J. Lee, Simple methods for tracking stem cells with (64)Cu-labeled DOTA-hexadecyl-benzoate, ACS Med. Chem. Lett. 6 (2015) 528–530.

[146] S.R. Lane, P. Nanda, T.L. Rold, G.L. Sieckman, S.D. Figueroa, T.J. Hoffman, S.S. Jurisson, C.J. Smith, Optimization, biological evaluation and microPET imaging of copper-64-labeled bombesin agonists, [^{64}Cu-NO2A-(X)-BBN(7-14)NH_2], in a prostate tumor xenografted mouse model, Nucl. Med. Biol. 37 (2010) 751–761.

[147] M.H. Kim, J.A. Park, S.-K. Woo, K.C. Lee, G.I. An, B.S. Kim, K.I. Kim, T.S. Lee, C.W. Kim, K.M. Kim, J.H. Kang, Y.J. Lee, Evaluation of a ^{64}Cu-labeled 1,4,7-triazacyclononane, 1-glutaric acid-4,7 acetic acid (NODAGA)-galactose-bombesin analogue as a PET imaging probe in a gastrin-releasing peptide receptor-expressing prostate cancer xenograft model, Int. J. Oncol. 46 (2015) 1159–1168.

[148] A.B. Jackson, P.K. Nanda, T.L. Rold, G.L. Sieckman, A.F. Szczodroski, T.J. Hoffman, X. Chen, C.J. Smith, ^{64}Cu-NO2A-RGD-Glu-6-Ahx-BBN(7-14)NH_2: a heterodimeric targeting vector for positron emission tomography imaging of prostate cancer, Nucl. Med. Biol. 39 (2012) 377–387.

[149] R. Bergmann, A. Ruffani, B. Graham, L. Spiccia, J. Steinbach, J. Pietzsch, H. Stephan, Synthesis and radiopharmacological evaluation of ^{64}Cu-labeled bombesin analogs featuring a bis(2-pyridylmethyl)-1,4,7-triazacyclononane chelator, Eur. J. Med. Chem. 70 (2013) 434–446.

[150] H. Guo, Y. Miao, Cu-64-labeled lactam bridge-cyclized alpha-MSH peptides for PET imaging of melanoma, Mol. Pharm. 9 (2012) 2322–2330.

[151] A.J. Chang, R. Sohn, Z.H. Lu, J.M. Arbeit, S.E. Lapi, Detection of rapalog-mediated therapeutic response in renal cancer xenografts using (64)Cu-bevacizumab immunoPET, PLoS One 8 (2013), e58949, https://doi.org/10.1371/journal.pone.0058949.

[152] A.F. O'Neill, J.L.J. Dearling, Y. Wang, T. Tupper, Y. Sun, J.C. Aster, M.L. Calicchio, A.R. Perez-Atayde, A.B. Packard, A.L. Kung, Targeted imaging of ewing sarcoma in preclinical models using a ^{64}Cu-labeled anti-CD99 antibody, Clin. Canc. Res. 20 (2014) 678–687.

[153] Y. Gai, L. Sun, W. Hui, Q. Ouyang, C.J. Anderson, G. Xiang, X. Ma, D. Zeng, New Bifunctional Chelator p-SCN-PhPr-NE3TA for Copper-64: synthesis, peptidomimetic conjugation, radiolabeling, and evaluation for pet imaging, Inorg. Chem. 55 (2016) 6892–6901.

[154] Y. Xiao, H. Hong, A. Javadi, J.W. Engle, W. Xu, Y. Yang, Y. Zhang, T.E. Barnhart, W. Cai, S. Gong, Multifunctional unimolecular micelles for cancer-targeted drug delivery and positron emission tomography imaging, Biomaterials 33 (2012) 3071–3082.

[155] J.E. Sprague, H. Kitaura, W. Zou, Y. Ye, S. Achilefu, K.N. Weilbaecher, S.L. Teitelbaum, C.J. Anderson, Noninvasive imaging of osteoclasts in parathyroid hormone-induced osteolysis using a ^{64}Cu-labeled RGD peptide, J. Nucl. Med. 48 (2007) 311–318.

[156] Y. Guo, R. Ferdani, C.J. Anderson, Preparation and biological evaluation of ^{64}Cu labeled Tyr 3-octreotate using a phosphonic acid-based cross-bridged macrocyclic chelator, Bioconjugate Chem. 23 (2012) 1470–1477.

[157] Z. Cai, Q. Ouyang, D. Zeng, K.N. Nguyen, J. Modi, L. Wang, A.G. White, B.E. Rogers, X.Q. Xie, C.J. Anderson, ^{64}Cu-labeled somatostatin analogues conjugated with cross-bridged phosphonate-based chelators via strain-promoted click chemistry for PET imaging: in silico through in vivo studies, J. Med. Chem. 57 (2014) 6019–6029.

[158] A. Kumar, G. Hao, L. Liu, S. Ramezani, J.T. Hsieh, O.K. Oz, X. Sun, Click-chemistry strategy for labeling antibodies with copper-64 via a cross-bridged tetraazamacrocyclic chelator scaffold, Bioconjugate Chem. 26 (2015) 782–789.

[159] D. Soodgupta, M.A. Hurchla, M. Jiang, A. Zheleznyak, K.N. Weilbaecher, C.J. Anderson, M.H. Tomasson, M. Shokeen, Very late antigen-4 ($\alpha_4\beta_1$ -integrin) targeted pet imaging of multiple myeloma, PLoS One 8 (2013), e55841, https://doi.org/10.1371/journal.pone.0055841.

[160] D. Zeng, Y. Guo, A.G. White, Z. Cai, J. Modi, R. Ferdani, C.J. Anderson, Comparison of conjugation strategies of cross-bridged macrocyclic chelators with cetuximab for copper-64 radiolabeling and PET imaging of EGFR in colorectal tumor-bearing mice, Mol. Pharm. 11 (2014) 3980–3987.

[161] N. Bhatt, N. Soni, Y.S. Ha, W. Lee, D.N. Pandya, S. Sarkar, J.Y. Kim, H. Lee, S.H. Kim, G.I. An, J. Yoo, Phosphonate pendant armed propylene cross-bridged cyclam: synthesis and evaluation as a chelator for Cu-64, ACS Med. Chem. Lett. 6 (2015) 1162–1166.

[162] A.V. Dale, G.I. An, D.N. Pandya, Y.S. Ha, N. Bhatt, N. Soni, H. Lee, H. Ahn, S. Sarkar, W. Lee, P.T. Huynh, J.Y. Kim, M.R. Gwon, S.H. Kim, J.G. Park, Y.R. Yoon, J. Yoo, Synthesis and evaluation of new generation cross-bridged bifunctional chelator for (64)Cu radiotracers, Inorg. Chem. 54 (2015) 8177–8186.

[163] B.M. Paterson, G. Buncic, L.E. McInnes, P. Roselt, C. Cullinane, D.S. Binns, C.M. Jeffery, R.I. Price, R.J. Hicks, P.S. Donnelly, Bifunctional (64)Cu-labelled macrobicyclic cage amine isothiocyanates for immuno-positron emission tomography, Dalton Trans. 44 (2015) 4901–4909.

[164] B.M. Paterson, K. Alt, C.M. Jeffery, R.I. Price, S. Jagdale, S. Rigby, C.C. Williams, K. Peter, C.E. Hagemeyer, P.S. Donnelly, Enzyme-mediated site-specific bioconjugation of metal complexes to proteins: Sortase-mediated coupling of copper-64 to a single-chain antibody, Angew. Chem. Int. Ed. 53 (2014) 6115–6119.

[165] K. Alt, B.M. Paterson, K. Ardipradja, C. Schieber, G. Buncic, B. Lim, S.S. Poniger, B. Jakoby, X. Wang, G.J. Okeefe, H.J. Tochon-Danguy, A.M. Scott, U. Ackermann, K. Peter, P.S. Donnelly, C.E. Hagemeyer, Single-Chain antibody conjugated to a cage amine chelator and labeled with positron-emitting copper-64 for diagnostic imaging of activated platelets, Mol. Pharm. 11 (2014) 2855–2863.

[166] M. Ziegler, K. Alt, B.M. Paterson, P. Kanellakis, A. Bobik, P.S. Donnelly, C.E. Hagemeyer, K. Peter, Highly sensitive detection of minimal cardiac ischemia using positron emission tomography imaging of activated platelets, Sci. Rep. 6 (2016) 6:38161, https://doi.org/10.38110.31038/srep38161.

[167] E. Gourni, L. Del Pozzo, E. Kheirallah, C. Smerling, B. Waser, J.-C. Reubi, B.M. Paterson, P.S. Donnelly, P.T. Meyer, H.R. Maecke, Copper-64 labeled macrobicyclic sarcophagine coupled to a GRP receptor antagonist shows great promise for pet imaging of prostate cancer, Mol. Pharm. 12 (2015) 2781–2790.

[168] K.A. Lears, R. Ferdani, K. Liang, A. Zheleznyak, R. Andrews, C.D. Sherman, S. Achilefu, C.J. Anderson, B.E. Rogers, In vitro and in vivo evaluation of ^{64}Cu-labeled SarAr-bombesin analogs in gastrin-releasing peptide receptor-expressing prostate cancer, J. Nucl. Med. 52 (2011) 470–477.

[169] B.M. Paterson, P. Roselt, D. Denoyer, C. Cullinane, D. Binns, W. Noonan, C.M. Jeffery, R.I. Price, J.M. White, R.J. Hicks, P.S. Donnelly, PET imaging of tumours with a ^{64}Cu labeled macrobicyclic cage amine ligand tethered to Tyr3-octreotate, Dalton Trans. 43 (2014) 1386–1396.

[170] S. Liu, D. Li, C.W. Huang, L.P. Yap, R. Park, H. Shan, Z. Li, P.S. Conti, The efficient synthesis and biological evaluation of novel bi-functionalized sarcophagine for (64)Cu radiopharmaceuticals, Theranostics 2 (2012) 589–596.

[171] G.L. DeNardo, D.L. Kukis, S. Shen, L.F. Mausner, C.F. Meares, S.C. Srivastava, L.A. Miers, S.J. DeNardo, Efficacy and toxicity of 67Cu-2IT-BAT-Lym-1 radioimmunoconjugate in mice implanted with human Burkitt's lymphoma (Raji), Clin. Canc. Res. 3 (1997) 71–79.

[172] G.L. Denardo, S.J. Denardo, D.L. Kukis, R.T. O'Donnell, S. Shen, D.S. Goldstein, L.A. Kroger, Q. Salako, D.A. Denardo, G.R. Mirick, L.F. Mausner, S.C. Srivastava, C.F. Meares, Maximum tolerated dose of ^{67}Cu-2IT-BAT-LYM-1 for fractionated radioimmunotherapy of non-Hodgkin's lymphoma: a pilot study, Anticancer Res. 18 (1998) 2779–2788.

[173] G.L. DeNardo, D.L. Kukis, S. Shen, D.A. DeNardo, C.F. Meares, S.J. DeNardo, ^{67}Cu- versus ^{131}I-labeled Lym-1 antibody: comparative pharmacokinetics and dosimetry in patients with non-Hodgkin's lymphoma, Clin. Canc. Res. 5 (1999) 533–541.

[174] G.R. Mirick, R.T. O'Donnell, S.J. Denardo, S. Shen, C.F. Meares, G.L. Denardo, Transfer of copper from a chelated ^{67}Cu-antibody conjugate to ceruloplasmin in lymphoma patients, Nucl. Med. Biol. 26 (1999) 841–845.

[175] Y. Sugo, K. Hashimoto, M. Kawabata, H. Saeki, S. Sato, K. Tsukada, Y. Nagai, Application of ^{67}Cu produced by ^{68}Zn(n,n'p+d)^{67}Cu to biodistribution study in tumor-bearing mice, J. Phys. Soc. Jap. 86 (2017), 023201-03.

[176] Z.H. Jin, T. Furukawa, T. Ohya, M. Degardin, A. Sugyo, A.B. Tsuji, Y. Fujibayashi, M.R. Zhang, T. Higashi, D. Boturyn, P. Dumy, T. Saga, 67Cu-Radiolabeling of a multimeric RGD peptide for $\alpha_v\beta_3$ integrin-targeted radionuclide therapy: stability, therapeutic efficacy, and safety studies in mice, Nucl. Med. Commun. 38 (2017) 347–355.

[177] D.S. Lee, H.J. Im, Y.S. Lee, Radionanomedicine: widened perspectives of molecular theragnosis, Nanomedicine 11 (2015) 795–810.

[178] E.K. Lim, T. Kim, S. Paik, S. Haam, Y.M. Huh, K. Lee, Nanomaterials for theranostics: recent advances and future challenges, Chem. Rev. 115 (2015) 327–394.

[179] H. Huang, J.F. Lovell, Advanced functional nanomaterials for theranostics, Adv. Funct. Mater. 27 (2017) 1–22, https://doi.org/10.1002/adfm.201603524.

[180] M.-C.Z. Abadjian, J. Choi, C.J. Anderson, Nanoparticles for PET imaging of tumors and cancer metastasis, in: J.W.M. Bulte, M.M.J. Modo (Eds.), Design and Applications of Nanoparticles in Biomedical Imaging, Springer Int. Publ., Switzerland, 2017, pp. 229–255.

[181] S.C. Ghosh, A. Azhdarinia, Advances in the development of multimodal imaging agents for nuclear/near-infrared fluorescence imaging, Curr. Med. Chem. 22 (2015) 3390–3404.

[182] J. Guo, H. Hong, G. Chen, S. Shi, Q. Zheng, Y. Zhang, C.P. Theuer, T.E. Barnhart, W. Cai, S. Gong, Image-guided and tumor-targeted drug delivery with radiolabeled unimolecular micelles, Biomaterials 34 (2013) 8323–8332.

[183] https://clinicaltrials.gov/ct2/show/NCT01304797, Safety and Pharmacokinetic Study of MM-302 in Patients With Advanced Breast Cancer.

[184] H. Lee, J. Zheng, D. Gaddy, K.D. Orcutt, S. Leonard, E. Geretti, J. Hesterman, C. Harwell, J. Hoppin, D.A. Jaffray, T. Wickham, B.S. Hendriks, D. Kirpotin, A gradient-loadable (64)Cu-chelator for quantifying tumor deposition kinetics of nanoliposomal therapeutics by positron emission tomography, Nanomedicine 11 (2015) 155–165.

[185] T.W. Liu, T.D. MacDonald, J. Shi, B.C. Wilson, G. Zheng, Intrinsically copper-64-labeled organic nanoparticles as radiotracers, Angew. Chem. Int. Ed. 51 (2012) 13128–13131.

[186] Y. Fazaeli, S. Feizi, A.R. Jalilian, A. Hejrani, Grafting of [(64)Cu]-TPPF20 porphyrin complex on Functionalized nano-porous MCM-41 silica as a potential cancer imaging agent, Appl. Radiat. Isot. 112 (2016) 13–19.

[187] L. Cui, Q. Lin, C.S. Jin, W. Jiang, H. Huang, L. Ding, N. Muhanna, J.C. Irish, F. Wang, J. Chen, G. Zheng, A PEGylation-Free biomimetic porphyrin nanoplatform for personalized cancer theranostics, ACS Nano 9 (2015) 4484–4495.

[188] P. Zhang, C. Hu, W. Ran, J. Meng, Q. Yin, Y. Li, Recent progress in light-triggered nanotheranostics for cancer treatment, Theranostics 6 (2016) 948–968.

[189] G. Ferro-Flores, B.E. Ocampo-Garcia, C.L. Santos-Cuevas, E. Morales-Avila, E. Azorin-Vega, Multifunctional radiolabeled nanoparticles for targeted therapy, Curr. Med. Chem. 21 (2014) 124–138.

[190] T. Liu, S. Shi, C. Liang, S. Shen, L. Cheng, C. Wang, X. Song, S. Goel, T.E. Barnhart, W. Cai, Z. Liu, Iron oxide decorated MoS_2 nanosheets with double PEGylation for chelator-free radiolabeling and multimodal imaging guided photothermal therapy, ACS Nano 9 (2015) 950–960.

[191] X. Sun, X. Huang, X. Yan, Y. Wang, J. Guo, O. Jacobson, D. Liu, L.P. Szajek, W. Zhu, G. Niu, D.O. Kiesewetter, S. Sun, X. Chen, Chelator-free ^{64}Cu-integrated gold nanomaterials for positron emission tomography imaging

guided photothermal cancer therapy, ACS Nano 8 (2014) 8438–8446.
[192] X. Sun, X. Huang, J. Guo, W. Zhu, Y. Ding, G. Niu, A. Wang, D.O. Kiesewetter, Z.L. Wang, S. Sun, X. Chen, Self-illuminating ^{64}Cu-doped CdSe/ZnS nanocrystals for in vivo tumor imaging, J. Am. Chem. Soc. 136 (2014) 1706–1709.
[193] Z. Wang, P. Huang, O. Jacobson, Z. Wang, Y. Liu, L. Lin, J. Lin, N. Lu, H. Zhang, R. Tian, G. Niu, G. Liu, X. Chen, Biomineralization-inspired synthesis of copper sulfide-ferritin nanocages as cancer theranostics, ACS Nano 10 (2016) 3453–3460.
[194] M. Zhou, Y. Chen, M. Adachi, X. Wen, B. Erwin, O. Mawlawi, S.Y. Lai, C. Li, Single agent nanoparticle for radiotherapy and radio-photothermal therapy in anaplastic thyroid cancer, Biomaterials 57 (2015) 41–49.
[195] Q. Feng, Y. Zhang, W. Zhang, Y. Hao, Y. Wang, H. Zhang, L. Hou, Z. Zhang, Programmed near-infrared light-responsive drug delivery system for combined magnetic tumor-targeting magnetic resonance imaging and chemo-phototherapy, Acta Biomater. 49 (2017) 402–413.
[196] H.H. Coenen, A.D. Gee, M. Adam, G. Antoni, C.S. Cutler, Y. Fujibayashi, J.M. Jeong, R.H. Mach, T.L. Mindt, V.W. Pike, A.D. Windhorst, Consensus nomenclature rules for radiopharmaceutical chemistry — setting the record straight, Nucl. Med. Biol. 55 (2017) v-xi.